Facies (2011) 57:51–72
DOI 10.1007/s10347-010-0229-x

ORIGINAL ARTICLE

Tectonically driven carbonate ramp evolution at the southern Tethyan shelf: the Lower Eocene succession of the Galala Mountains, Egypt

Stefan Höntzsch · Christian Scheibner · Jochen Kuss · Akmal M. Marzouk · Michael W. Rasser

Received: 16 December 2009 / Accepted: 14 August 2010 / Published online: 14 September 2010

Abstract The succession of the Galala Mountains at the southern Tethyan margin (Eastern Desert, Egypt) provides new data for the evolution of an isolated carbonate platform in the Early Eocene. Since the Late Cretaceous emergence of the Galala platform, its evolution has been controlled strongly by eustatic sea-level fluctuations and the tectonic activity along the Syrian Arc-Fold-Belt. Previous studies introduced five platform stages to describe platform evolution from the Maastrichtian (stage A) to the latest Paleocene shift from a platform to ramp morphology (stage E). A first Early Eocene stage F was tentatively introduced but not described in detail. In this study, we continue the work at the Galala platform, focussing on Early Eocene platform evolution, microfacies analysis and the distribution of larger benthic foraminifera on a south-dipping inner ramp to basin transect. We redefine the tentative platform stage F and introduce two new platform stages (stage G and H) by means of the distribution of 13 facies types and syn-depositional tectonism. In the earliest Eocene (stage F, NP 9b–NP 11), facies patterns indicate mainly aggradation of the ramp system. The first occurrence of isolated sandstone beds at the mid ramp reflects a post-Paleocene-Eocene thermal maximum (PETM) reactivation of a Cretaceous fault system, yielding to the tectonic uplift of Mesozoic and Palaeozoic siliciclastics. As a consequence, the Paleocene ramp with pure carbonate deposition shifted to a mixed carbonate-siliciclastic system during stage F. The subsequent platform stage G (NP 11–NP 14a) is characterised by a deepening trend at the mid ramp, resulting in the retrogradation of the platform. The increasing deposition of quartz-rich sandstones at the mid ramp reflects the enhanced erosion of Mesozoic and Palaeozoic deposits. In contrast to the deepening trend at the mid ramp, the deposition of cyclic tidalites reflects a coeval shallowing and the temporarily subaerial exposure of inner ramp environments. This oppositional trend is related to the continuing uplift along the Syrian Arc-Fold-Belt in stage G. Platform stage H (NP 14a–?) demonstrates the termination of Syrian Arc uplift and the recovery from a mixed siliciclastic carbonate platform to pure carbonate deposition.

Keywords Egypt · Galala · Early Eocene · Isolated carbonate platform · Microfacies · Larger benthic foraminifera · Tectonism

S. Höntzsch (✉) · C. Scheibner · J. Kuss
Department of Geosciences, Bremen University,
PO Box 330440, 28359 Bremen, Germany
e-mail: stefanho@uni-bremen.de

A. M. Marzouk
Geology Department, Faculty of Science,
Tanta University, Tanta 31527, Egypt

M. W. Rasser
Staatliches Museum für Naturkunde,
Rosenstein 1, 70191 Stuttgart, Germany

Introduction

The evolution of circum-Tethyan carbonate platform systems during the Early Paleogene greenhouse has been studied intensively in recent decades with respect to environmental conditions (e.g. Luterbacher 1984; Kuss 1986; Rasser 1994; Wielandt 1996; Pujalte et al. 1999; Scheibner et al. 2001a; Cosovic et al. 2004; Özgen-Erdem et al. 2005; Rasser et al. 2005; Adabi et al. 2008), shallow-benthic biostratigraphy (e.g. Schaub 1992; Serra-Kiel et al. 1998; Scheibner and Speijer 2009), oil potential (e.g. Loucks et al. 1998; Ahlbrandt 2001; Baaske et al. 2008)

and the response to long- and short-term palaeoclimatic change (e.g. Scheibner et al. 2005, 2007; Pujalte et al. 2009; summary by Scheibner and Speijer 2008, and references therein). Major biotic platform contributors (e.g. corals, larger benthic foraminifera, calcareous green and red algae) play an important role in terms of the interpretation of environmental conditions and the evolution of the platform through time. Scheibner et al. (2005) compare various Early Palaeogene Tethyan carbonate platforms and arrange three circum-Tethyan platform stages (stage I–III) with respect to the main biotic contributors: in the Late Paleocene platform stage I (58.9–56.2 Ma) corals and calcareous algae dominate carbonate platforms all over the Tethys (coralgal platforms). Platform stage II (56.2–55.5 Ma) is characterised by the first occurrence of larger benthic foraminifera shoals at low latitudes (below 20°N), while coralgal assemblages prevail at high latitudes (above 30°N). In platform stage III (55.5 Ma–?), corals were replaced by larger benthic foraminifera (LBF) as major platform contributors in nearly all circum-Tethyan shallow-marine environments. The onset of platform stage III is coupled strongly to the environmental and sedimentological impact of the Paleocene-Eocene thermal maximum (PETM) at 55.5 Ma, resulting in the rapid radiation and proliferation of LBF species. This larger foraminifera turnover (LFT) also demonstrates the transition from Paleocene LBF assemblages (e.g. *Ranikothalia*, *Miscellanea*) to Eocene LBF assemblages (e.g. *Nummulites*, *Alveolina*, *Operculina*, *Orbitolites*), which are characterised by larger test sizes and adult dimorphism (e.g. Hottinger and Schaub 1960; Hottinger 1998; Orue-Etxebarria et al. 2001; Scheibner and Speijer 2009). Despite the well-known onset of platform stage III, its duration is still under debate. Multiple local circum-Tethyan studies are needed to reveal timing and trigger mechanisms with respect to the termination of platform stage III.

Additionally, the circum-Tethyan platform stages proposed by Scheibner et al. (2005) are based exclusively on climatically controlled biotic changes, while individual platform environments are affected by multiple regional factors regarding their position on the shelf and local tectonic constraints. The importance of tectonically controlled carbonate platform evolution has been described for various environments throughout the Phanerozoic (e.g. Lee Wilson and D'Argenio 1982; Burchette 1988; Bechstädt and Boni 1989; Bosence 2005). In the Early Eocene, the Egyptian shelf is especially strongly affected by tectonism, which is related to the northward movement of the African craton towards Eurasia as well as the reactivation of Mesozoic fault systems (e.g. Shahar 1994; Moustafa and Khalil 1995; Hussein and Abd-Allah 2001). Thus, the evolution of carbonate platforms at the Egyptian shelf is controlled by those tectonic constraints and requires a regional approach beyond the general platform stages of Scheibner et al. (2005).

The Galala Mountains (Eastern Desert, Egypt) represent a key area of Cenozoic carbonate platform research. Since the mid-1980s, investigations in the Galala Mountains have focussed on Cretaceous to Paleocene microfacies, platform evolution, palaeoecology and the impact of the PETM (e.g. Kuss 1986; Bandel and Kuss 1987; Strougo and Faris 1993; Kuss et al. 2000; Scheibner et al. 2001a, 2003; Morsi and Scheibner 2009).

The evolution of the Galala platform is coupled strongly to the activity of the Syrian Arc-Fold-Belt, which demonstrates a NE–SW striking framework of horst and graben structures at the southern Tethyan shelf. The Syrian Arc-Fold-Belt was formed as a result of the initial collision of the African and Eurasian Plates in the Late Turonian (e.g. Moustafa and Khalil 1995; Scheibner et al. 2003). The emergence of the Galala platform has been documented for the Campanian/Maastrichtian (Scheibner et al. 2003). Multiple pulses of tectonic uplift, which are related to the temporarily reactivation of Cretaceous fault systems, caused the repeated reconfiguration of the platform morphology. A major interval of tectonic uplift along the Syrian Arc-Fold-Belt is demonstrated for the Early Eocene (e.g. Shahar 1994).

Scheibner et al. (2003) discriminate five regional platform stages (stage A–E) from the Maastrichtian emergence of the platform system (stage A) to latest Paleocene prior to the PETM (stage E). Scheibner and Speijer (2008) introduced a sixth platform stage F, which is, however, neither defined in detail nor biostratigraphically classified.

Here, we present new data from the Galala Mountains that help to reveal the evolution of the platform system in the Early Eocene. We focus on detailed microfacies analyses, larger foraminifera assemblages and the effects of syn-depositional tectonic activity on carbonate platform sedimentation. Following the studies of Scheibner et al. (2003) and Scheibner and Speijer (2008), we redefine and reevaluate the tentative introduced platform stage F. Furthermore, we introduce two new platform stages (stage G and H) that delineate the evolution of the Galala carbonate platform in the Early Eocene. Both stages G and H demonstrate major incisions in platform evolution, characterised by varying tectono-sedimentary and biotic conditions, as well as the transition from global greenhouse climate to increased cooling at the end of the Early Eocene Climatic Optimum (EECO).

Geological setting

The Galala Mountains are located in the Eastern Desert of Egypt and range from Ain Sukhna near Suez 100 km to

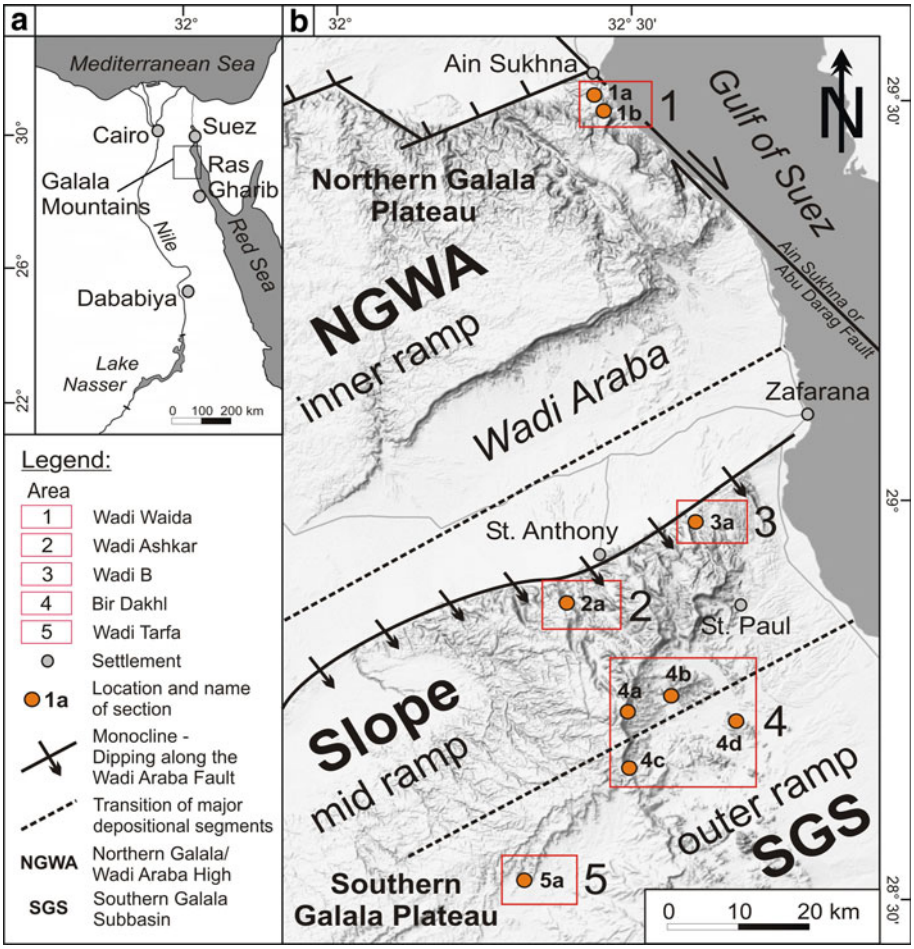

Fig. 1 **a** Simplified location map of the working area. **b** Detailed map with location of the sections, tectono-topographic features as well as the general facies belts of the carbonate platform (modified from Scheibner et al. 2001a). Tectonic elements are added according Moustafa and El-Rey (1993), Moustafa and Khalil (1995) and Schütz (1994)

the SE (Fig. 1). The mountain complex represents an isolated Late Cretaceous (Maastrichtian) to Eocene carbonate platform at the southern margin of the Tethys, which is referred to as the unstable shelf of northern Egypt (Youssef 2003; Fig. 2b). The evolution of the platform is connected closely to the tectonic activity of the ENE–WSW striking Wadi Araba Fault, which forms part of the Syrian Arc-Fold-Belt (e.g. Krenkel 1925; Moustafa and Khalil 1995; Hussein and Abd-Allah 2001). During the Early Eocene, a major phase of tectonic activity occured along the Syrian Arc-Fold-Belt (Shahar 1994). Regional uplift and subsidence triggered the formation of ENE–WSW striking basins, submarine swells and subaerially exposed plateaus on the unstable shelf (Said 1990; Schütz 1994; Fig. 2b). Major plateaus are situated in the Cairo-Suez- and Kattamiya area as well as on the present-day coast of the Mediterranean Sea. The regional basins had a width of a few tens to hundreds of kilometres, with a palaeobathymetry of about 100 m (Salem 1976). However, the basinal succession of the stable shelf south of the study area comprises a palaeobathymetry of up to 600 m (Speijer and Wagner 2002).

The Early Eocene Galala Mountains represent one of the southernmost plateaus of the Egyptian unstable shelf (Fig. 2b). According to regional tectono-sedimentary constraints, three major depositional units can be distinguished (Fig. 1b): the Northern Galala/Wadi Araba High (NGWA), a transitional slope zone, and the Southern Galala Subbasin (SGS). The NGWA represents shallow-marine to probably subaerially exposed inner platform environments. Due to the synsedimentary monoclinal uplift and following erosion along the Wadi Araba Fault since the Late Cretaceous, major inner-ramp deposits were eroded or intensively altered (Moustafa and Khalil 1995). Furthermore, rocks of the northern platform interior are intensively affected by secondary dolomitisation and tectonic displacement, which is a result of the Miocene opening of the Gulf of Suez. The connection between the NGWA and the SGS is represented by a transitional slope zone (mid ramp to outer ramp). The Galala Mountains are tectonically and depositionally linked to the monoclinal structure of Gebel Somar on west-central Sinai (Moustafa and Khalil 1995). Both structures were separated during the rifting of the Gulf of Suez in the Late Oligocene and Miocene.

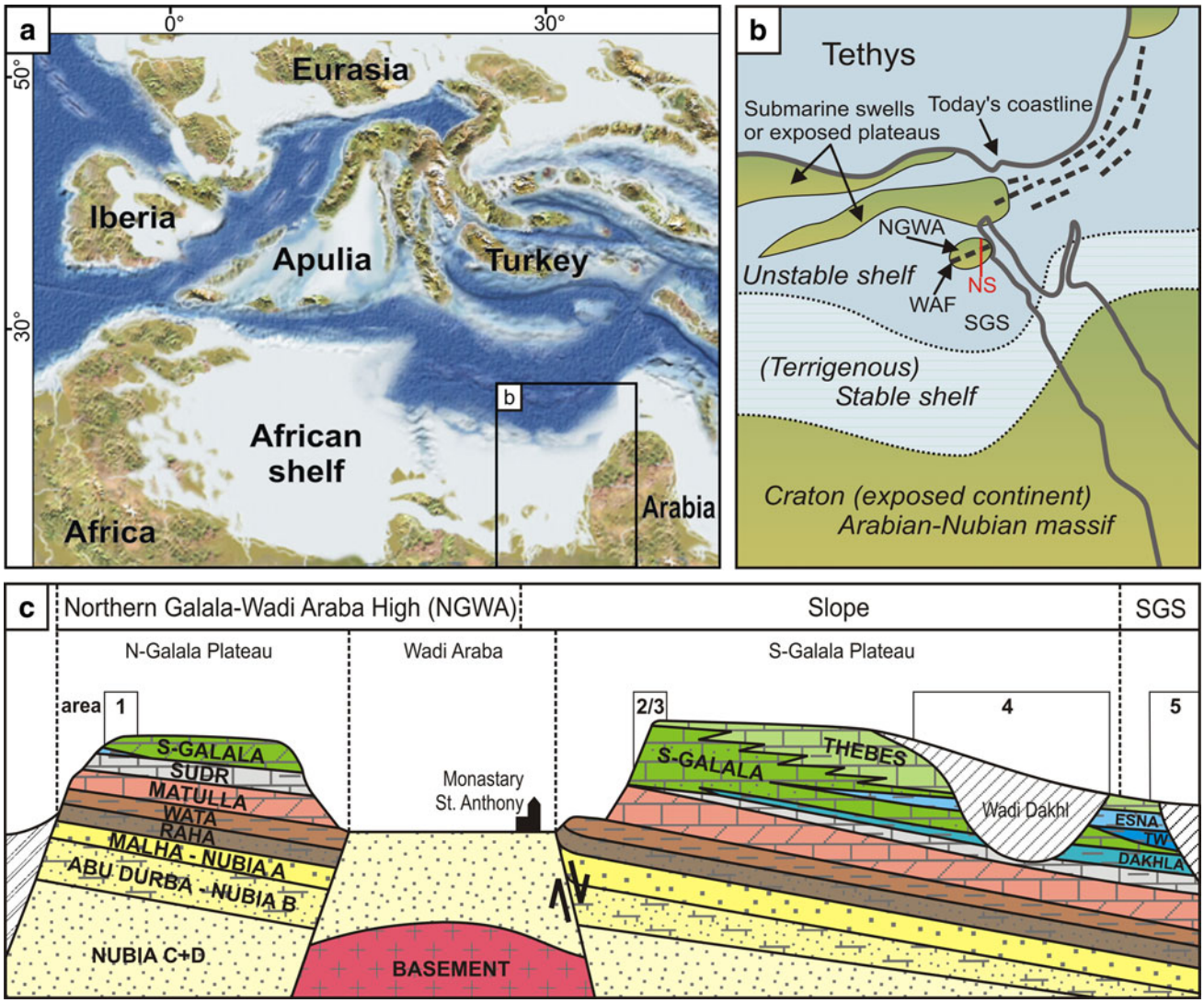

Fig. 2 **a** Palaeogeographic overview of the western Tethyan realm in the earliest Palaeogene using the maps of Blakey (http://jan.ucc.nau.edu/~drcb7/latecretmed.jpg). **b** Simplified map of the Early Eocene southern Tethys margin in Egypt showing the location of the Northern Galala/Wadi Araba High (*NGWA*) and the Southern Galala Subbasin (*SGS*). The Wadi Araba Fault (*WAF*) forms the southern part of the Syrian Arc-Fold-Belt (*dashed lines*). Submarine swells and plateaus are added according to Said (1990) and Schütz (1994). The position of stable and unstable shelf was estimated by Meshref (1990) and was modified for the Early Palaeogene by Scheibner et al. (2001a, b) and Speijer and Wagner (2002). The red line (*NS*) represents an NS-directed cross-section shown in **c**. **c** Cross-section of the Galala Mountains including the working areas (numbers 1, 2/3, 4 and 5) and main formations (modified from Schütz 1994). Palaeozoic to Lower Cretaceous siliciclastics are represented by the Nubia Series. The Upper Cretaceous is dominated by siliciclastic marls, shales and (dolomitic) limestones (Wata, Raha, Matulla). The Sudr Formation represents the uppermost Cretaceous in the study area. Palaeogene formations (Dakhla, Tarawan, Esna, Southern Galala, Thebes) are diachronous. Their stratigraphic range is discussed in Fig. 3

Lithostratigraphy

The Lower Eocene succession in the Galala Mountains encompasses three major lithostratigraphic units, which differ in their stratigraphic range and varying depositional setting within an inner platform to basin transect (Figs. 2c, 3): The Esna Formation (Beadnell 1905) represents an interval of uppermost Paleocene to Lower Eocene basinal marls and shales (lower NP 9 to NP 12). The deposits lack shallow-marine influence and represent a palaeo-depth of 200 m on average (Speijer and Schmitz 1998; Scheibner et al. 2001a; Fig. 1b). The Esna Formation is followed by alternating chalky marls, cherts and sandstones of the Thebes Formation (Hermina and Lindenberg 1989), which represents a deep-water facies. Lithostratigraphically, the Thebes Formation is defined by the first appearance of cherts in the mid ramp to basinal sections, coinciding roughly with the initial occurrence of chalky marls in the Lower Eocene succession of the Galala Mountains (see Fig. 1b).

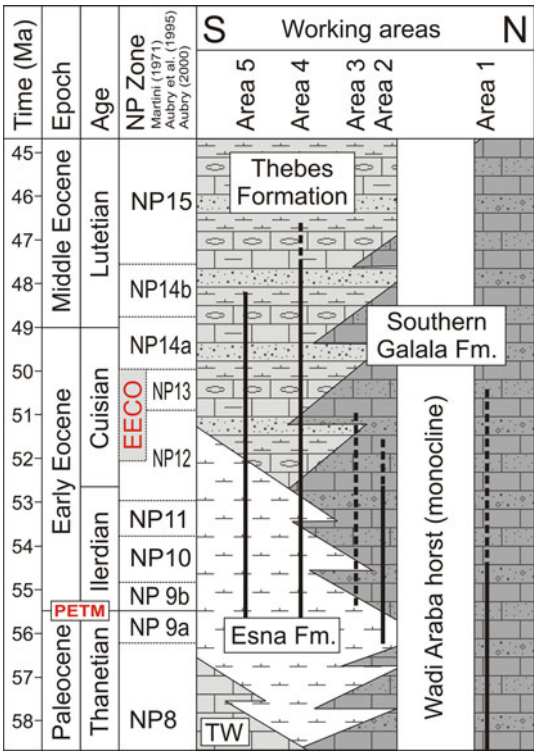

Fig. 3 Lithostratigraphy and biostratigraphy of the Palaeogene formations and groups in the Galala Mountains along a N–S transect (after Scheibner et al. 2001a, b; see Fig. 2c). The working areas (1–5) refer to Fig. 1b; position of Paleocene-Eocene thermal maximum (PETM) and Early Eocene Climatic Optimum (EECO) according to Zachos et al. (2008). *TW* Tarawan formation. *Vertical bold lines* Stratigraphic range of the recorded sections, *dashed lines* uncertain range

Marly sediments are rare or absent in the shallow-marine inner- to mid-ramp environments of the study area. The succession consists of platform-related, shallow-marine limestones, sandstones and conglomerates, which are represented by the Southern Galala Formation (Abdallah et al. 1970; Kuss and Leppig 1989). Thebes Formation and Southern Galala Formation show distinct facies similarities and interfinger at different areas on the mid ramp (Scheibner et al. 2001a).

Methods

Nine stratigraphical sections, located on a platform to basin transect between Ain Sukhna and Ras Ghareb in the Galala Mountains were measured in detail (Fig. 1): two exposures in the NGWA (area 1), four exposures covering the slope (area 2, 3 and 4) and three exposures in the SGS (area 4 and 5). The distance between the studied sections at the Southern Galala Plateau varies between 5 and 20 km. The thickness of the sections ranges from 70 m (section 3a) to 250 m (section 4a). The vertical sample distance varies between 20 cm in well-exposed marls to more than 1 m in sandstones, depending on the general condition of the outcrop and the degree of alteration. About 600 samples were taken for detailed thin section analysis of mainly litho- and biofacies. Thirteen facies types (FT) were defined according to the distribution and the assemblages of bioclasts (smaller and larger benthic foraminifera, planktic foraminifera, calcareous green and coralline red algae), matrix composition (micrite, sparite, dolomite) and quartz content. The classification of FT and facies belts (FB) follows previous studies of Paleocene successions (e.g. Scheibner et al. 2001a). Quantitative analysis was performed by estimation of components, using the comparison charts of Baccelle and Bosellini (1965) and Schäfer (1969), which provide reasonably quantitative results.

The detailed biostratigraphic assessment of the sections is based on calcareous nannoplankton (nannoplankton zonation of Martini 1971; Aubry 1995; Aubry et al. 2000). Shallow-platform biostratigraphy was supported by alveolines according to the classification of Hottinger (1974) and the shallow-benthic zonation (SBZ) of Serra-Kiel et al. (1998) and Scheibner and Speijer (2009).

Results and facies interpretation

Description and biostratigraphic range of the sections

The nine studied sections represent different depositional environments along a NNE–SSW striking ramp (Figs. 1, 2c). A clear proximal–distal zonation is evident from the northern inner ramp (area 1) to the southern ramp-basin transition (area 4) and finally to the southern most basinal area 5.

The Paleocene-Eocene boundary is defined by the transition from NP 9a to NP 9b and the transition from SBZ 4 to SBZ 5, and coincides with the carbon isotope excursion (CIE) of the PETM (Scheibner et al. 2005; Scheibner and Speijer 2009). The studied sections range from NP 9 to NP 14a, whilst the lowermost Middle Eocene sections are within NP 14b. A continuous biostratigraphic assessment of the respective shallow benthic zones (SBZ 6 to SBZ 13) was hindered by poorly preserved specimen in all intervals.

Area 1

The deposits of the inner ramp are characterized by alternating limestones and reworked dolostones. Marls are rare or absent. The thickness of the individual sections ranges from 110 m (section 1a) to 125 m (section 1b). The biota are dominated by larger and smaller benthic foraminifera

(smaller miliolids, soritids, nummulitids, alveolinids) and green and red algae. The basal part of section 1b shows an alternating succession of LBF floatstones and fine-grained dolostones, which become more dominant towards the middle interval of the section. The upper portions of section 1b are represented by the cyclic deposition of fossiliferous dolostones (soritids, green algae, molluscs), birdseyes limestones and reworked limestone conglomerates (Fig. 7). Stratigraphically, section 1a ranges from the Paleocene to NP 10. The basal 40 m of section 1b cover the lowermost Eocene (NP 9b–NP 10). A biostratigraphic assessment of the subsequent 85 m of dolomitic rocks was not possible due to lacking biostratigraphic markers.

Area 2/3

The proximal mid ramp deposits of the northern margin of the Southern Galala Plateau are represented by a mixture of highly fossiliferous sandstones and limestones, marls and dolostones. Section 2a is composed by quartz-rich allochthonous peloidal limestones with intercalated sandstones and marls. Quartz-rich sandstones and conglomerates of section 2a are poorly sorted and show high amounts of limestone and sandstone extraclasts. Strong bioturbation is common as well as sharp contacts with the underlying beds. The lower 140 m of section 3a are composed of a marly sandstone-limestone succession. Sandstones prevail as sheet-like beds or as channelised structures with strongly varying thickness. Dolostones prevail in the upper 110 m of section 3a with monotonous and almost non-fossiliferous mud- to wackestones as well as massive beds of dolomitized nummulitic float- to rudstones. Stratigraphically, section 3a ranges from the uppermost Paleocene (NP 9a) to the upper Lower Eocene (NP 13/14). Section 2a covers the lowermost Eocene NP 9b–NP 10/11).

Area 4

The four studied sections of area 4 (4a, 4b, 4c and 4d) are dominated by marls (up to 45 m thick) with intercalated sandstones and limestones. The thickness of the sandstones varies between 1 cm and more than 3 m (section 4a). The greyish to bluish marls of the lower part of the sections (Esna Formation) are replaced by white chalky marls with frequent chert nodules towards the top of the succession (Thebes Formation). Intercalated limestone beds, which are present in the lower part of the succession, decrease towards the top. Dominant components are represented by LBF, benthic green algae, shell fragments and planktic foraminifera. Biostratigraphically, the sections of area 4 range from the uppermost Paleocene (NP 9a) to the uppermost Lower Eocene (NP 14a).

Area 5

The rocks of section 5a are characterised by greyish marls and shales in the lower interval (NP 9a–NP 11) and white chalky marls with high amounts of planktic foraminifera and radiolaria as well as intercalated chert bands in the upper part of the succession (NP 11–NP 14). Limestones or sandstones as well as larger benthic biota are absent. The total thickness of section 5a is about 90 m.

Facies types

The studied rocks are attributed to 13 FT, reflecting depositional settings on a ramp from shallow-marine (FT 1) to deep-marine environments (FT 13). For the distinction of FT, microfacies data as well as field observations of sedimentary structures are used (Table 1). Description and interpretation of the FT is based mainly on the high-diverse fauna of the shallow-marine, low-latitude succession of the Galala platform (Fig. 4). All 13 FT were attributed to five major facies belts (FB) on an inner ramp to basin transect (Fig. 5): (1) restricted lagoon, (2) inner lagoon, (3) outer lagoon and shoal, (4) slope, (5) toe-of-slope and basin.

Reworked dolostones (FT 1)

Description: FT 1 is represented by a suite of massive to parallel-bedded light grey dolostones with layers of dark grey to black birdseyes and fenestral textures (Fig. 4a, q), followed by coarse-grained crystalline dolostones with reworked birdseyes mudstones, which are arranged in a coarsening upward succession. The individual beds have a thickness of a few centimetres up to more than 2 m. Biogenic remains are generally rare or absent. Occasionally extraclasts enriched in corals and gastropods, as well as stromatolithic textures occur in the reworked beds (e.g. bed W2-12). Desiccation cracks are present in bed W2-14 (Fig. 4q). The thickness of the individual cycles varies between 50 cm and more than 10 m. The thickness of the conglomerates on top of each cycle ranges from 5 to 20 cm; rarely up to 2 m. FT 1 is present only in section 1b and covers the upper 70 m of the succession.
Interpretation: FT 1 reflects the shallowest part of the restricted Galala platform. The succession of fossil-barren, completely altered birdseyes mudstone followed by reworked conglomerates indicates cyclicity of a tidal flat facies (Keheila and El-Ayyat 1990). Desiccation cracks reveal periodically subaerial exposure.

Dolomitised mudstones to wackestones (FT 2)

Description: FT 2 is represented either by massive, grey dolostones with almost no macroscopic textures or by

Table 1 Summary of facies types (FT) for the studied sections, including occurrence, main components, texture, quartz content and interpretation of the environment. *FB* Facies belt

Number	FT	Sub FT	Occurrence, area	Main components[d]	Quartz	Texture	Environment, FB
1	Reworked dolostones		1	–	–	Massive to parallel-bedded, fenestral textures, birdseyes	Restricted inner ramp/lagoon
2	Dolomitised mudstones to wackestones		1	Rare bioclasts	Rare, common in one sample	Massive to nodular	Restricted inner ramp/lagoon
3	Peloidal packstones to grainstones		1, 2, 3, 4	Peloids, miliolids, green algae	Rare-common	Massive to parallel-bedded	Inner ramp, restricted lagoon
4	Gastropod-rich bioclastic wackestones to packstones		1.3	Gastropods, *Alveolina*, serpulids, peloids	Rare, common in one sample	Massive, partly stromatolithic	Inner ramp, lagoon
5	Nummulitid-bioclastic wackestones to packstones		1, 2, 3, 4	Small *Nummulites*, miliolids, peloids, small bioclasts	Few (<10%)	Parallel-bedded to massive	Inner ramp, semi-restricted lagoon
6	Dasyclad-rich soritid floatstones		1	Green algae, *Orbitolites*	–	Thin-bedded	Inner ramp, sheltered backshoal/lagoon
7	Red algae bindstones		One sample in area 3	Red algae (*Sporolithon*)	–	Stromatolithic	Inner ramp/lagoon
8	Alveolinid-green algal wackestones to floatstones		1, 2, 3, 4	*Alveolina*, green algae, miliolids, peloids	Rare to common (<40%)	Massive to parallel-bedded	Inner ramp, sheltered backshoal/lagoon
9	Nummulitid-alveolinid wackestones to floatstones		Floatstones: 1, packstones: 2, 3, 4	Large and small *Nummulites*, *Alveolina*, green algae	Common	Massive	Inner- to mid ramp, (back)shoal
10	Nummulitid floatstones to sandstones	a	1, 3, 4	Large and small *Nummulites*	Common	Massive	Upper mid ramp, shoal
		b	3.4	*Ranikothalia*, *Miscellanea*	Rare	Massive	Upper mid ramp, shoal
		c	3.4	*Assilina*, *Operculina*	Rare to common	Massive	Upper mid ramp, shoal
11	(Conglomeratic) quartz sandstones		2, 3, 4	–	Common	Massive to parallel-bedded, fining-upward	Mid ramp, slope
12	Bioclastic wackestones to packstones		2, 3, 4	Small bioclasts, *Discocyclina*, planktic foraminifera, peloids	Rare to common	Massive	Mid ramp, slope
13	Planktic foraminiferal and radiolaria-rich wackestones to packstones	a	3, 4, 5	Planktic foraminifera	–	Massive to parallel-bedded	Mid- to outer ramp, slope
		b	4.5	Radiolarians, planktic foraminifera	–	Parallel-bedded to massive	Deeper mid- to outer ramp, slope to toe-of-slope

[d] Main components and organisms are listed in order of decreasing abundance

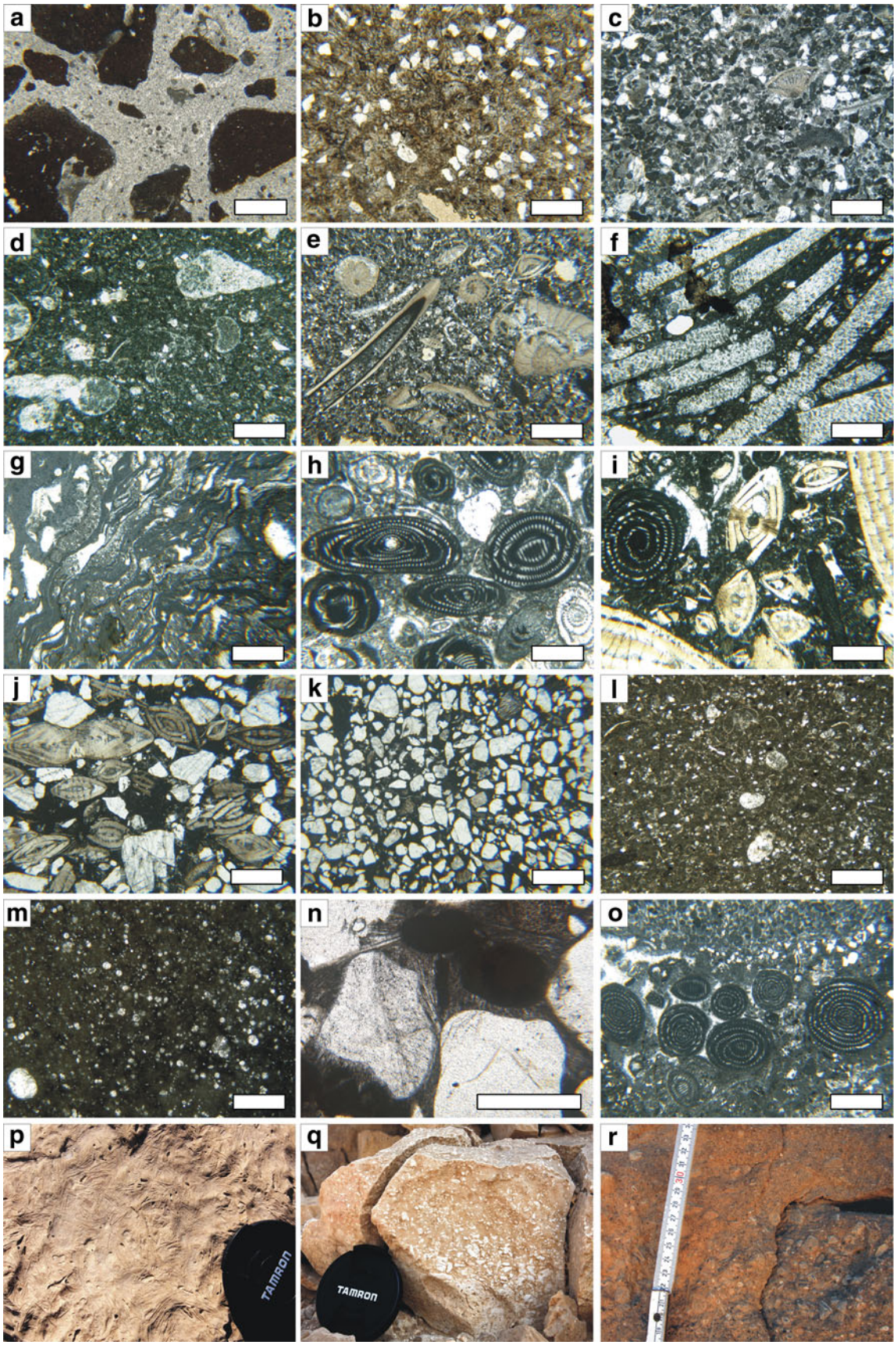
a
b
c
d
e
f
g
h
i
j
k
l
m
n
o
p
q
r
TAMRON
TAMRON

◀ **Fig. 4a–r** Facies types (FT) of the studied Eocene strata. **a** Reworked dolostones (FT 1), **b** dolomitised mudstones to wackestones (FT 2) with well-sorted quartz grains and rare bioclasts, **c** Peloidal packstones to grainstones (FT 3) with abundant smaller lenticular nummulitids and miliolids, **d** gastropod-rich bioclastic wackestones to packstones (FT 4), **e** nummulitid-bioclastic wackestones to packstones (FT 5) with peloids and rare serpulid worm tubes, **f** dasyclad-rich soritid floatstones (FT 6), **g** red algal bindstones (FT 7) consisting almost exclusively of non-geniculate red algae *Sporolithon* sp., **h** alveolinid-green algal wackestones to floatstones (FT 8) with common silicified *Alveolina* sp. specimen, **i** nummulitid-alveolinid wackestones to floatstones (FT 9). Note the common eroded outer whorls of the *Alveolina* specimen. Nummulites are only rarely affected by erosion, **j** nummulitid floatstones to sandstones (FT 10) with abundant immature quartz grains, **k** (conglomeratic) quartz sandstones (FT 11) with a high maturity and a muddy matrix, **l** bioclastic wackestones to packstones (FT 12) dominated by planktic foraminifera and smaller bioclasts, **m** planktic foraminiferal radiolaria-rich wackestones to packstones (FT 13), **n** radial fibrous cements in FT 4, **o** subtype of FT 6 with infraformational conglomerate composed of alveolinids, **p** weathered surface texture showing soritids and green algal relics (FT 8 in section 1b), **q** fenestral texture within dolomitised mudstones (FT 2, section 1b), **r** fining upward sequence of a debris flow in section 4a, note the high abundance of LBF. *Bars* 1 mm

reworked nodules with remains of corals, gastropods and stromatolitic textures within FT 1 (Fig. 4b). Dolomite is present as inequigranular and non-rhombic crystals. Relics of miliolids and ostracods are rare. Fragments of alveolinids and smaller nummulitids are intensively affected by dolomitisation. Siliciclastic material is generally absent; only few samples contain up to 20% of well-sorted, subangular quartz grains (e.g. bed W2-10). Massive and coarsely recrystallised wackestones often occur in the northern part of the study area (area 1).

Interpretation: Dolomitised mudstones with very rare faunal elements occur in restricted environments of the inner ramp. Stromatolites indicate very shallow water conditions with temporarily subaerial exposure. Dolomitisation is thought to be late diagenetic and related to hypersaline brines of a tidal flat (Keheila and El-Ayyat 1992). Samples with quartz and extraclasts probably reflect reworking by occasional storm events.

Peloidal packstones to grainstones (FT 3)

Description: Light to dark grey peloidal pack- to grainstones occur as massive or parallel-bedded limestones with sharp contacts to adjacent beds. Lumps densely packed peloids dominating this FT, the latter with volume percentages of 25–50% (Fig. 4c). Dominant components are milio-

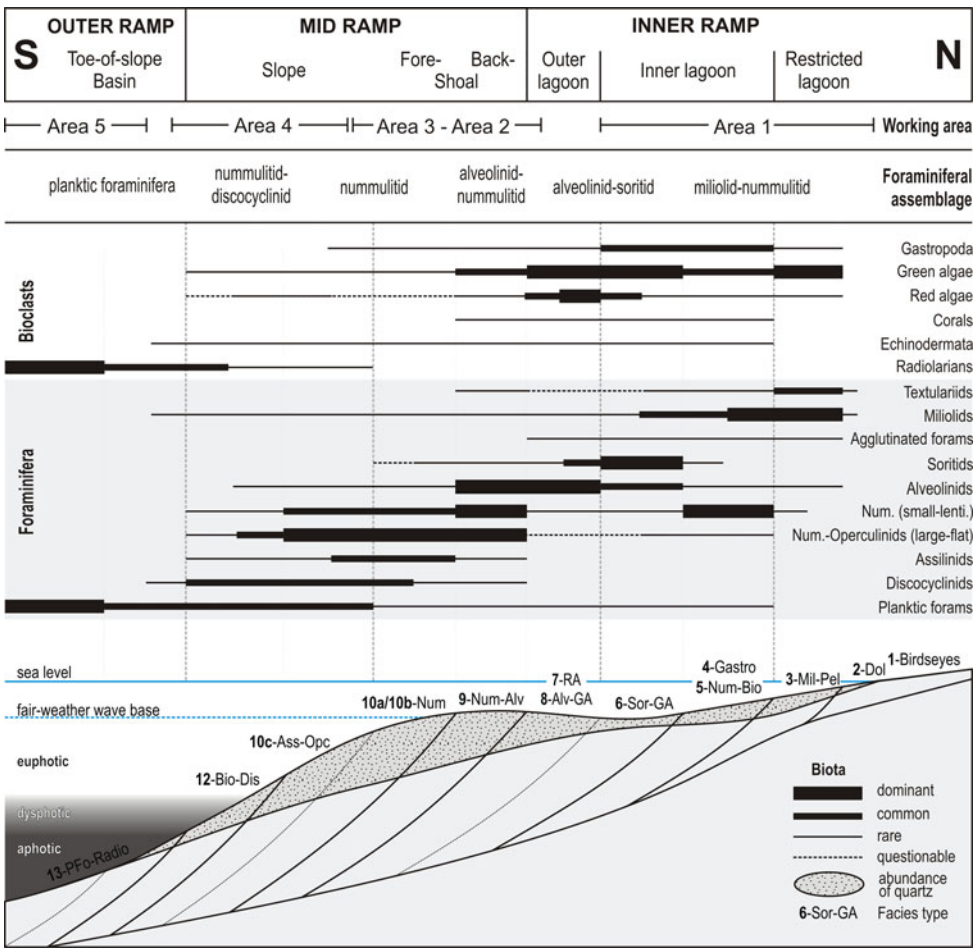

Fig. 5 Semi-quantitative distribution of the main microfossils combined with six foraminiferal assemblages and facies types (FT 1–10, 12, 13) on the Galala platform. *PFo* Planktic foraminifera, *Radio* radiolarians, *Bio* bioclastic, *Dis* discocyclinids, *Ass* assilinids, *Num* nummulitids, *Opc* operculinids, *Alv* alveolinids, *GA* green algae, *RA* red algae, *Sor* soritids, *Gastro* gastropods, *Mil* miliolids, *Pel* peloids, *Dol* dolomite, *lenti.* lenticular. FT 11 (conglomeratic quartz sandstone) is not plotted and is supposed to occur on a wide range of nearly all palaeoenvironments in the study area. The discrimination of inner-, mid- and outer ramp environments with the help of different bioclasts and larger foraminifera is demonstrated only roughly due to the lack of in situ deposits in the study area

lids (>15%) and micritised green algal fragments. Smaller lenticular nummulitids, alveolinids, red algae, corals and textulariids are subordinate. Quartz occurs generally from rare to common. The matrix consists of xenotopic microsparite and rarely blocky sparite. Micritic parts of the matrix occur in isolated patches. Peloidal packstones to grainstones often interfinger with other FT (e.g. nummulitid-bioclast wackestones to packstones). This FT occurs in all sections of the study area except in area 5.
Interpretation: FT 3 reflects shallow inner ramp environments. The common sparry matrix with patches of micrite and the good sorting of the components indicates high-hydrodynamic conditions and reworking. Most peloids are interpreted as micritised fragments of green algae or smaller benthic foraminifera (e.g. miliolids). Recent miliolids dominate shallow-marine lagoonal environments (e.g. Murray 1991). It is reported, that those foraminifera are capable of tolerating high salinities and also proliferate as epiphaunal benthos within seagrass communities (e.g. Davies 1970; Murray 1991). Palaeoenvironmental studies on miliolid assemblages attribute the low diversity of the detected foraminifera associated with common green algal fragments to nutrient-enriched conditions in a restricted environment (e.g. Geel 2000; Zamagni et al. 2008).

Gastropod-rich bioclastic wackestones to packstones (FT 4)

Description: The wacke- to packstones of FT 4 are present as massive light grey to bluish-grey limestones with a thickness of 10–50 cm. Besides the frequent gastropods, fragments of alveolinids, peloids, serpulid worm tubes and miliolids occur with various ratios (Fig. 4d). FT 4 occurs occasionally in areas 1 and 3. In section 3a (bed B5-31), quartz and peloids occur as major components. In section 1b, traces of microbial stromatolitic textures are present (bed W2-12).
Interpretation: The faunal assemblage of FT 4 reflects inner ramp environments with close relations to FT 3 and FT 5. Gastropod-rich bioclastic wacke- to packstones represent shallow lagoonal conditions with moderate water circulation above fair-weather wave base (Scheibner et al. 2007). Quartz and peloids are probably storm-derived.

Nummulitid-bioclastic wackestones to packstones (FT 5)

Description: Nummulitic-bioclastic wacke- to packstones are represented by parallel-bedded or massive, grey to yellow rocks with a thickness between 10 cm and more than 1 m. This FT is characterised by an inhomogenic assemblage of smaller lenticular *Nummulites* sp., miliolids, textulariids, alveolinids, benthic green algae and peloids (Fig. 4e). Smaller quartz grains are present with minor amounts (<10%). The matrix consists of micrite or microsparite; in section 1b, FT 5 is strongly dolomitised. FT 5 occurs frequently in area 1, 2, 3 and 4.
Interpretation: FT 5 represents inner ramp environments above fair-weather wave base. The faunal assemblage reflects semi-restricted lagoonal conditions with a moderate water circulation. The occurrence of peloids and quartz grains indicates a mixture with other FT. Thus, FT 5 either occurs as in situ deposit at the inner ramp or as allochthonous remains in deeper realms of the ramp (e.g. section 4b).

Dasyclad-rich soritid floatstones (FT 6)

Description: Floatstones of FT 6 are represented by micritic grey to bluish-grey limestones with a bimodal distribution of elongated soritids (*Orbitolites* sp., *Opertorbitolites* sp.) and oval-to-round green algal fragments (mostly Dasycladacean algae). Both components make up to 55% of the whole rock volume (Fig. 4f, p). Other biogenic components, as shell fragments are generally rare. FT 6 occurs only on top of section 1b (area 1).
Interpretation: The low-diverse assemblage of benthic green algae and elongated soritids, as well as the absence of quartz suggest low-hydrodynamic conditions in well-flushed backreef or backshoal environments (Hottinger 1973, 1997; Geel 2000). Zamagni et al. (2008) interpret the patchy cooccurrence of green algae and soritids as evidence for the existence of algal meadows. Recent relatives of Palaeogene soritids proliferate in sheltered environments with 0–40 m water depth (Geel 2000).

Red algae bindstones (FT 7)

Description: FT 7 occurs in dark grey to bluish-grey limestones with a stromatolitic texture. Fossil remains are represented by non-geniculate coralline red algae (*Sporolithon* sp. >50%) as well as rare shell and green algal fragments. Red algal thalli accumulate in laminated beds with a thickness between 500 µm and 2 mm (Fig. 4g). FT 7 is present only in section 3a as extraclasts within a 160-cm-thick interval of alveolinid sandstones (FT 8, bed B1-50).
Interpretation: Coralline red algae bindstones occur as small patch reefs in the deeper protected inner ramp below fair-weather wave base (e.g. Gietl 1998; Scheibner et al. 2007). The occurrence of FT 7 as extraclasts within a suite of coarse-grained alveolinid-rich sandstones suggests a deposition in the vicinity of the inner- to mid ramp transition. Gietl (1998) describes red algal patch reefs at the southern margin of the Northern Galala Plateau, reflecting an inner ramp environment. The erosion of inner ramp material containing coralline red algal bindstones is possibly related to local tectonic displacement or dramatic storm events, resulting in isolated debris flows or large-scale slumps.

Alveolinid-green algal wackestones to floatstones (FT 8)

Description: FT 8 is arranged in massive to parallel-bedded grey to bluish-grey lime- and sandstones with a thickness between 20 and 150 cm. Alveolinids (up to 50%) and benthic green algae (up to 40%) are the dominant components (Fig. 4h). Peloids and miliolids are generally common and occur in various ratios and assemblages. Nummulitids, red algae (e.g. *Distychoplax biserialis*), shells and echinoderm fragments as well as *Orbitolites* are present in a minor extent. Quartz is frequent in the upper mid ramp sections (area 3, up to 40%) but rare in the NGWA (area 1).

One sample (B1-4, Fig. 4o) shows a limestone conglomerate with oval-shaped extraclasts enriched in peloids and green algal fragments. Between the individual extraclasts strongly abraded alveolinids occur. The matrix is primarily sparry with local patches of micrite.

Interpretation: Alveolinids and benthic green algae are typical components of the proximal low-energetic inner ramp (Scheibner et al. 2007). The occurrence of soritids supports an environment within sheltered lagoonal or backshoal settings (Hottinger 1973; Zamagni et al. 2008). High amounts of quartz in the vicinity of the platform margin possibly represent an allochthonous equivalent of this facies, which was reworked and transported into deeper settings (e.g. Papazzoni and Trevisani 2006).

Nummulitid-alveolinid wackestones to floatstones (FT 9)

Description: Yellow-grey limestones, which occur as massive beds with sharp but with undulating base and top surfaces, are summarised in FT 9. Stratification is generally rare, whereas fining-upward gradation occurs occasionally. *Nummulites* sp. and *Alveolina* sp. dominate this FT reaching 20–40% volume percentage (Fig. 4i). Other components are benthic green algae and quartz (5–30%); one sample is enriched in peloids. Miliolids, serpulid worm tubes, discoclyclinids and echinoderm fragments are present with lower percentages. The tests of all foraminifera are abraded. Especially alveolinids are often broken or squeezed. Few specimen show a strong abrasion of the outer whorls and probably lack their adult stages. Other LBF specimen show partial silicification. The poorly sorted quartz grains are generally sub-angular to sub-rounded. Micrite is the prevailing matrix of FT 9, which is replaced by sparite in a few samples. In section 1a, FT 9 is frequently dolomitised with idiotopic euhedral dolomite crystals. Generally, FT 9 is one of the most frequent facies types in the study area. Floatstones occur mostly in area 1, whereas wacke- to packstones are common in the southern study areas (area 3 and 4).

Interpretation: FT 9 represents high-energy shoals (backshoal) formed at the inner/mid ramp transition. This is also evidenced by the co-occurrence of alveolinids and nummulitids, reflecting a mixing of inner- and mid ramp environments (Hohenegger et al. 1999). Immature quartz grains indicate only minor transport fractionation, whereas the eroded tests of larger foraminifera and patches of sparry cement indicate stronger currents. However, the occurrence of FT 9 at the mid ramp sections of area 4 (e.g. section 4a) is related to the transport by major mass-flows. The silicification of LBF results from diagenetic alteration (Papazzoni and Trevisani 2006), when calcite is replaced by autigenic silica (mostly microcrystalline quartz). Silica originates from the dissolution of biogenic material (e.g. radiolarians; see FT 13b).

Nummulitid floatstones to sandstones (FT 10)

Description: The massive, yellow-grey beds of FT 10 commonly show a sharp basis. Larger elongated nummulitids with particularly high amounts of quartz dominate this FT (Fig. 4j). In contrast to other FT, miliolids and alveolinids are rare or absent. Quartz grains are poorly to moderately sorted; the sub-angular to sub-spherical grains are up to 5 mm in diameter. Discocyclinids, smaller rotaliids, alveolinids, echinoderm and bivalve shell fragments as well as other biogenic remains are present in varying amounts and preservations. Partial damage and deformation of larger foraminiferal tests is common and intensified with increasing quartz content. The matrix consists of micrite or microsparite. In a few samples, quartz grains are overgrown by radial fibrous cements (bed D5-149; Fig. 3n). Nummulitid floatstones to sandstones are common in area 3 and 4. Lenticular beds with a thickness of a few metres are present in area 1.

FT 10 shows various microfacies types: 10a-dominated by *Nummulites* sp., 10b-dominated by *Ranikothalia* sp. and *Miscellanea* sp., 10c-dominated by *Assilina* sp. and *Operculina* sp.

Interpretation: FT 10 represents mixed-energetic deposits of the upper mid ramp, which were probably transported due to occasional storm events below fair-weather wave base. However, the poor sorting indicates only minor transport. *Discocyclina* sp., *Assilina* sp. and *Operculina* sp. point to a neritic environment with a water depth between 50 m and 80 m (microfacies type 10c, Beavington-Penney and Racey 2004). True convex-shaped or lenticular shoal deposits, which are typical at the platform margin, are present only in the NGWA (area 1). Radial fibrous cement indicates high agitation and low sedimentation rates (Lighty 1985). In the Paleocene interval of section 4a the dominating major nummulitids are represented by *Ranikothalia* sp. and *Miscellanea* sp. (subtype b), which indicate the same environment as *Nummulites* sp. (subtype a).

(Conglomeratic) quartz sandstones (FT 11)

Description: FT 11 is represented by a suite of light grey to yellow, mostly monomineralic quartz sandstones with a varying maturity (Fig. 4k). Rocks are massive or parallel bedded and cross stratification is rare. The thickness of the individual beds varies between 2 mm (e.g. section 4c) and several metres (e.g. section 3a). The basis of the beds is frequently undulated but sharp. Rip-up clasts of subsequent beds are common (e.g. marls). Occasionally, fining-upward is present in parallel-bedded sandstones. The sorting of the siliciclastics is generally moderate to good; the sphericity of the quartz grains is poor to moderate. The size of the individual grains ranges from 100 µm to 3 mm. A decrease in maturity is noticeable in rocks with higher amounts of coarser grains. The matrix contains mud or is completely washed out. Relics of glauconite and weathered feldspar, as well as peloids are rare. Nummulitids, alveolinids, planktic foraminifera, bivalve shells and green algal fragments are generally rare and occur abraded or fragmented. Low fossiliferous quartz sandstones occur in a wide range in almost all sections of the study area. FT 11 is absent only in areas 1 and 5.
Interpretation: Massive to parallel bedded sandstones indicate moderate to high-hydrodynamic conditions. High amounts of siliciclastic material were probably eroded due to uplift along the Wadi Araba Fault. Sediment transport was possibly triggered by storm events or local tectonic activity (e.g. earthquakes). Massive bedding results from intensified bioturbation (Reineck and Singh 1980), dewatering of the sediment during diagenesis (Förstner et al. 1968) or the intensified activity of microorganisms (Werner 1963). The lack of biogenic material indicates either the transport of fossil-barren material from a point source or an intensified destruction of larger shelled biota. However, the lack of palaeoenvironmental indicators hinders the classification of FT 11 at the ramp. The occurrence of quartz sandstones at the upper and lower mid ramp suggests a source area in the vicinity of the NGWA. The repeated deposition of sandstone beds probably reflects the transport in existent distal channels or incised valleys at the mid ramp.

Bioclastic wackestones to packstones (FT 12)

Description: Bluish-grey to dark grey micritic limestones of FT 12 (Fig. 4l) demonstrate an inhomogeneous assemblage of densely packed aggregated grains and smaller bioclasts (miliolids, smaller rotaliids, green and red algal fragments, discocyclinids and planktic foraminifera). Peloids are present in minor amounts (rarely 25%). Well-sorted, sub-angular to sub-sphaeric quartz grains are common in section 4a (10–20%) and occur occasionally in area 3 as major component (bed B5-31, ~30%). The size of the quartz grains varies between 50 and 300 µm. Elongated nummulitids, assilinids and discocyclinids "float" as larger components in the fine-grained matrix. The matrix consists of mud or microsparite. FT 12 is recorded in all studied areas, with the exception of area 1 and 5.
Interpretation: Multicomponent bioclastic wackestones to packstones are interpreted as distal debris flows or turbidites, which consist of reworked material from the inner ramp (e.g. miliolids, green algae) as well as authochthonous deeper ramp biota (e.g. discocyclinids). The co-occurrence of planktic foraminifera and discocyclinids point to a deposition at the dysphotic lower mid ramp. Bassi (1998) describes large *Discocyclina* assemblages across the inner and mid ramp transition. Good sorting and the small size of the major components indicate an advanced fractionation by transport.

Planktic foraminiferal and radiolaria-rich wackestones to packstones (FT 13)

Description: FT 13 shows two subtypes: FT 13a—light to bluish grey planktic foraminiferal wackestones are represented by massive or parallel bedded limestones and chalky marls. The individual beds have a thickness of between 30 cm up to 1 m and show no or only vague parallel stratification. FT 13a is enriched in planktic foraminifera (up to 30%); other fossil groups, such as radiolarians or ostracods, are generally rare (Fig. 3m). Biogenic material is enriched in layers of a few millimetres to centimetres or in clotted aggregates. FT 13a occurs particularly in the southern part of the study area (area 4 and 5), as well as in extraclasts in debris flow deposits in area 3.

FT 13b—Parallel bedded, laminated or massive white chalky marls and limestones represent another subtype of FT 13. The rocks are dominated by radiolarians and planktic foraminifera. A micritic matrix is generally absent. The occurrence of nodular to banded cherts with accumulated radiolarian and planktic foraminiferal remains characterises this subtype of FT 13. Chert nodules show an elongated oval shape with a thickness of 5–20 cm. Limestones and marls that are dominated by radiolarians occur in area 4 and 5.
Interpretation: Planktic foraminiferal and radiolaria-rich wackestones to packstones are interpreted as typical low-hydrodynamic deep water deposits of the lower mid- to outer ramp with no or minor terrigenous input. Beds with accumulated planktic organisms indicate more condensed conditions or transient blooms. Clotted nests of planktic foraminifera and radiolarians reflect bioturbation. Chert nodules of the Lower Eocene Drunka and Thebes Formation are interpreted as product of post-depositional meteoric alteration due to shelf progradation in the Early Eocene (e.g. Keheila and El-Ayyat 1990; McBride et al. 1999).

Foraminiferal assemblages

The following six foraminiferal assemblages are arranged on a palaeobathymetric profile, ranging from the shallow-marine inner ramp to the deep-marine basin (Fig. 5): (1) miliolid assemblage, (2) alveolinid assemblage, (3) nummulitid-alveolinid assemblage, (4) nummulitid assemblage, (5) nummulitid-discocyclinid assemblage and (6) planktic foraminifera assemblage.

The transitions between the individual foraminiferal assemblages are gradual and occasionally interfere with each other.

Assemblage 1: Miliolid assemblage

Description: This assemblage is dominated by smaller porcellaneous miliolids and small lenticular nummulitids. Assemblage 1 is associated with benthic red and green algae (e.g. dasycladaceans), textulariids and smaller alveolinids. Rare faunal components are echinoderm and bivalve shell fragments, as well as gastropods. The miliolid facies is common in area 2 and 3, as well as in sections 4a and 4b of area 4.
Interpretation: The dominance of miliolids and the absence of larger flattened foraminifera indicate a very shallow-marine setting of a restricted lagoon (inner ramp). Recent miliolid species prefer euryhaline, low-hydrodynamic environments on soft substrates (e.g. Murray 1991). The association with abundant green algae fragments and smaller rotaliids reflect the occurrence of algal meadows and elevated nutrient levels in the shallow lagoon (Davies 1970).

Assemblage 2: Alveolinid assemblage

Description: The alveolinid assemblage is characterised by the major occurrence of larger miliolid foraminifera (e.g. *Alveolina* sp.). Assemblage 2 is associated with soritids, benthic green algae and smaller miliolids. Minor bioclasts are represented by bivalve shell fragments, gastropods, discocyclinids, nummulitids, echinoderm remains and planktic foraminifera. The tests of the LBF are generally well preserved and show only occasionally abraded adult whorls. Assemblage 2 occurs in sections 2a, 3a, 4a and 4b.
Interpretation: Assemblage 2 represents illuminated shallow-water environments at the open-marine inner to upper mid ramp, characterized by low water turbulence. Dominant LBF (*Alveolina* sp., *Orbitolites* sp., *Opertorbitolites* sp.) proliferate in algal meadows (e.g. Dill et al. 2007). The occurrence of green algae and heterotrophic grazers (e.g. gastropods) indicates elevated nutrient levels.

Assemblage 3: Nummulitid-alveolinid assemblage

Description: Assemblage 3 is dominated by the cooccurrence of *Nummulites* sp. and *Alveolina* sp. *Nummulites* occur as large flattened specimens as well as small lenticular forms. Benthic green algae occur occasionally as a major component. Other bioclasts are generally rare. In the Paleocene intervals of the studied sections, foraminiferal assemblage 3 is characterised by the dominance of *Ranikothalia* sp., *Miscellanea* sp. and *Glomalveolina* sp., which demonstrate the precursors of *Nummulites* sp. and *Alveolina* sp. This assemblage occurs in sections 1a, 1b, 2a and 3a and occasionally in section 4a.
Interpretation: Most of the recent alveolinids and nummulitids prevail in various environments on a carbonate ramp (Hohenegger et al. 1999). Alveolinids proliferate on the protected inner ramp within seagrass communities, whereas nummulitids can occur on a wide range at the platform. Large-flattened fossil nummulitids dominate the deeper parts of the ramp or occur at the seaward side of shoals, whereas small-lenticular forms live together with alveolinids in more protected inner ramp environments (e.g. Geel 2000). The coeval occurrence of large-flat nummulitids and alveolinids, reflecting two different environments either point to an offshore transport of alveolinids (Adabi et al. 2008) or to a shoal-to-inner ramp transport of nummulitids.

Assemblage 4: Nummulitid assemblage

Description: The nummulitid assemblage is characterized by the cooccurrence of large-flattened and small, lenticular forms of *Nummulites* sp. Occasionally, forms of *Assilina* sp. are present as a major component. Operculinids, discocyclinids and smaller bioclasts are rare or absent. Nummulitid-dominated rocks occur in sections 3a, 4a and rarely in section 4b.
Interpretation: Small, lenticular nummulitids reflect favourable environmental conditions, resulting in a high and quick reproduction rate but small test size (Hallock and Glenn 1986; Beavington-Penney and Racey 2004). Favourable conditions prevail in well-lighted shallow-marine (<20 m) inner ramp environments with good food supply and moderate- to high water agitation. Larger flattened nummulitids are adapted to unfavourable light or food conditions at deeper parts of the ramp (Hallock 1985). Quick reproduction is replaced by a continuing growth of the tests. The co-occurrence of small-lenticular and larger-elongated specimen concludes the post-depositional transport of shallow inner-ramp forms (small-lenticular) towards deeper realms of the ramp.

Assemblage 5: Nummulitid-discocyclinid assemblage

Description: Foraminiferal assemblage 5 is dominated by large and flat orthophragminids (*Discocyclina* sp.) and various species of nummulitids (*Operculina* sp., *Nummulites* sp., *Assilina* sp.). Planktic and agglutinated foraminifera, smaller miliolids and rotaliids as well as green and red algal fragments occur in variable amounts. The tests of the LBF show a moderate to good preservation. Adult whorls are only occasionally abraded. Assemblage 5 is present in area 4 and rarely in area 2 and 3.
Interpretation: Large flat nummulitids and orthophragminids reflect an environment in the lower euphotic to upper dysphotic zone up to 130 m water depth (Racey 1994; Cosovic and Drobne 1995; Zamagni et al. 2008) where decreasing light intensity requires larger test surfaces to host photo-autotrophic organisms. Flattened LBF indicate an environment with marly to sandy substrates (Zamagni et al. 2008). Notwithstanding, assilinids, operculinids and *Nummulites* can occur in the same environment, they are supposed to be dominant in different depths in the water column. Their cooccurrence in few mid ramp sections (area 4) indicates the relocation of shallower deposits towards deeper realms. Summarising, foraminiferal assemblage 5 was deposited in the euphotic to dysphotic mid ramp below fair-weather wave base.

Assemblage 6: Planktic foraminifera assemblage

Description: Assemblage 6 consists nearly exclusively of planktic foraminifera and radiolaria. Ostracods and smaller benthic foraminifera are rare. The low-diverse community of foraminiferal assemblage 6 occurs in all studied areas.
Interpretation: High amounts of planktic organisms and the coeval absence of storm-derived inner ramp-related bioclasts, indicate distal authochtonous depositional environments below the storm wave base. The absence of photo-autotrophic benthos (LBF, green algae) reflects aphotic conditions at the sea-floor. For tropical marine environments without major terrigenous input a depositional palaeo-water depth below 100 m, which corresponds to the distal mid- to outer ramp is suggested (Hohenegger 2005; Renema 2006).

Discussion

Platform evolution

Formation and evolution of carbonate platform systems are strongly controlled by eustatic sea-level changes and the activity of adjacent tectonic provinces (Bosellini 1989; Everts 1991). Based on the Paleocene record of the Galala platform, Scheibner et al. (2003) assume a platform evolution that is affected more by local tectonic displacements than by eustatically controlled sea-level changes. Thus, the tectonic activity along the Wadi Araba Fault system triggered the initial growth of the Galala platform as a coupled effect of sea-level drop and local tectonic uplift. Furthermore, the geometry and architecture of platform and slope have undergone repeated changes since the Cretaceous due to the varying tectono-sedimentary constraints on the unstable Egyptian shelf (Meshref 1990; Schütz 1994; Youssef 2003).

Scheibner et al. (2003) documented five platform stages regarding progradation and retrogradation of the platform margin, which encompasses the evolution of the study area from the Maastrichtian to the earliest Eocene (stages A–E, Fig. 8). Stages A and B describe the transition between hemipelagic and slope deposition, reflecting the initial stages (Maastrichtian to Late Paleocene, NP 5). The first progradational phase of the Galala platform is documented in the Late Paleocene (NP 5 to NP 6, stage C), which is related to uplift along the Wadi Araba Fault and a major sea-level drop. A second progradational phase (stage D) occurred during NP 7 to NP 8. Massive debris flows filled up the accommodation space at the platform rim and forced a southward shift of the platform margin. Stage E represents platform retrogradation within the latest Paleocene (NP 9) up to the PETM, reflecting a sea-level rise. Retrogradation is accompanied by the widespread deposition of marls and the onset of LBF shoals on the platform margin. Within NP 9 the slope gradient decreased, due to the subsidence of the platform interior and the coeval uplift of the SGS.

Scheibner and Speijer (2008) introduced a sixth platform stage F, which is characterised by the first occurrence of *Nummulites* and *Alveolina* in the Galala succession. The base of stage F is represented by the PETM interval, which coincides with the larger foraminifera turnover and the Paleocene–Eocene boundary (boundary NP 9a–NP 9b). The post-PETM evolution of the Galala platform is characterised by a transitional phase of aggradation. Marls and allochthonous marly limestones dominate the deposition at the slope. In NP 10 the deposition of siliciclastics increased significantly, which indicates a reactivation of the Wadi Araba Fault.

Platform stage F is terminated within NP 11, due to several fundamental shifts regarding the tectonic constraints and the trophic regime in the depositional record of the Galala Mountains. Thus, we are introducing a seventh platform stage G. The initiation of stage G coincides approximately with the onset of the Thebes Formation in area 4 (~NP 11/12). The evolution of the Galala platform in the newly introduced stage G is characterised by the ongoing retrogradation with a coeval significant increase of

the tectonic activity along the Wadi Araba Fault. At least five major tectonic pulses, which are related to the uplift along the Wadi Araba Fault, are detected by means of the massive relocation of siliciclastic material and intervals with large slumping structures at the mid ramp. However, the lateral extension and distribution of siliciclastics at the ramp is highly heterogeneous, probably related to erosion and amalgamation of individual sandstone beds on the one hand, and the undulating slope topography that resulted from local tectonic uplift and subsidence on the other hand. The frequent occurrence of sandstone and conglomerate beds at the ramp margin (area 2 and 3) probably reflects the filling of ancient channel structures that were initialised during prior progradational stages (stage C and D). Large-scale slumps and frequent mass flows at the mid ramp (area 3 and 4) may indicate the onset of a distally steepened ramp, either within stage G or the upper part of stage F. A continuing deepening in stage G that coincides with retrogradation of the southern ramp margin is demonstrated by the increasing deposition of widespread chalky marls with chert nodules and increasing amounts of planktic foraminifera and radiolaria at the former slope (area 4). Furthermore, a significant shift in the microfacies composition from shallower to deeper signatures is evidenced for areas 3 and 4 within NP 11 (Fig. 7).

In contrast to the described scenarios for the areas 3 and 4, inner ramp sections (area 1) do not show any evidence of a major sea-level rise during the same intervals (Fig. 7). This contradiction possibly results from a coeval tectonic uplift of a horst structure (NGWA), which represents the inner ramp, and a continuing sea-level rise prior to the EECO (~NP 12/13, 52–50 Ma, Zachos et al. 2001). Tidal related loferite cycles in area 1 indicate very shallow and temporarily subaerial exposed conditions in the restricted platform interior (Bandel and Kuss 1987). Thus, the shallow inner-ramp areas widen during the sustained sea-level rise, while the mid ramp starts to drown. However, the gradient of the slope does not show any evidence of steepening during the Early Eocene. Palaeo-water depths for Paleocene intrashelf basins in Egypt (e.g. the SGS) were interpreted as being between 100 and 200 m (Salem 1976; Speijer and Wagner 2002). A homoclinal carbonate ramp with a slope of 100 km length would imply an average slope gradient of 0.02°. Thus, the increased deposition of mass-flows (debris flows, turbidites, slumps) must be related to local (tectonic) swells associated with steeper gradients or to a distally steepened ramp configuration. Furthermore, the facies signature of the mid ramp sections (area 4) indicate a deepening upward from the earliest Eocene (NP 10) to the uppermost Lower Eocene (NP 14a), which is manifested by decreasing proportions of inner- to mid ramp-related bioclasts (e.g. miliolids, peloids), forming mass-flow deposits. This deepening corresponds to the global transgression in the Early Eocene, which terminates in the highest sea level in the Cenozoic (e.g. Haq et al. 1987; Rea et al. 1990; Zachos et al. 1994; Miller et al. 2005). In contrast to Scheibner et al. (2000), who interpreted the occurrence of Paleocene mass-flows as a consequence of a major sea-level drop and ramp progradation, similar processes can be excluded for the Early Eocene. Evidence for the tectonic control of the shallowing at NGWA is the continuing deposition of siliciclastic material at the mid ramp throughout stage G.

The termination of stage G is evidenced within NP 14a (uppermost Early Eocene), due to a significant decrease in the tectonic-related deposition of siliciclastics. Especially in area 4 (sections 4a and 4b), the deposition of monotonous chalky chert-bearing marls without major sandstone and limestone beds demonstrates a reversal in the tectonic regime and the onset of a new platform stage, which we call stage H. Thus, sediments provided from the Wadi Araba horst were almost completely eroded and no inner ramp deposits are transported towards the SGS. Quartz-free mass flow deposits are rarely observed on top of the sections 4a and 4c. Here, well-sorted nummulitic pack- to floatstones probably indicate allochthonous equivalents of upper mid ramp LBF shoals. The exact stratigraphic range of stage H will be subject to further studies.

The dominance of larger benthic foraminifera as major platform contributing organisms suggests the continuation of the circum-Tethyan platform stage III of Scheibner et al. (2005) until NP 14a (~49 Ma). Our data do not indicate a recovery of major coral assemblages, which is related to a continuing warming trend throughout the Early Eocene, culminating during the EECO (53–49 Ma). A post-EECO cooling favours the recovery of temperature-controlled coral proliferation. However, post-EECO cooling has particularly affected high latitudes, whereas equatorial ocean basins remained warm throughout the Eocene (Tripati et al. 2003; Pearson et al. 2007). Thus, additional studies from Tethyan carbonate platforms at higher latitudes (e.g. Spain) are needed to demonstrate the impact of post-EECO cooling on platform organisms and to reveal the duration of circum-Tethyan platform stage III.

Tectonic constraints and the source of quartz

Quartz is generally rare in the Cretaceous and almost absent in the Paleocene of the Galala succession. Quartz-free carbonate mass-flow deposits were reported for the Late Paleocene, reflecting a massive sea-level drop during NP 5 (Lüning et al. 1998; Scheibner et al. 2000; Fig. 8a–d). Scheibner et al. (2003) describe first siliciclastic deposits in the latest Paleocene (NP 9a) and assume a source in the hinterland. During the Early Eocene, the abundance and frequence of sandstones and quartz-rich limestones

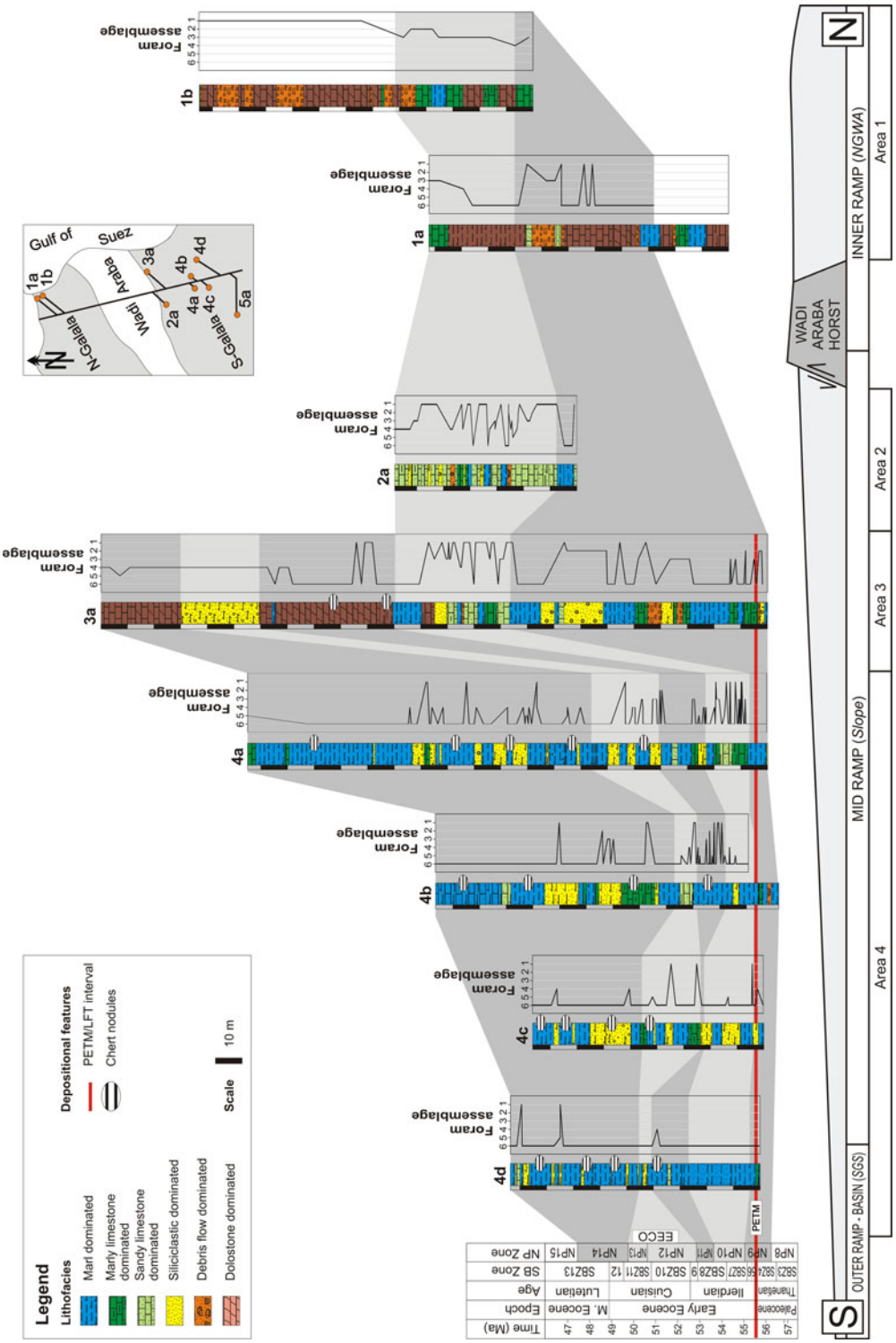

Fig. 6 Summary of all investigated sections, including the general lithofacies, foraminiferal assemblages and the biostratigraphic correlation based on calcareous nannoplankton. The arrangement of the sections on the lateral inner ramp to basin transect is shown in the small map to the right to the legend. The basis of all sections is the PETM/larger foraminifera turnover (LFT) interval (NP 9a–NP 9b boundary). The correlation of the NGWA (area 1) and the section of the Southern Galala Plateau (area 2 to area 5) is in question, due to the assumed asymmetric tectonic activity of the Wadi Araba horst and due to erosion of major upper environments. The block diagram below the sections illustrates the regional palaeogeographic context and the position of the sections at the ramp. Generally, autochthonous inner ramp habitats (lagoon, tidal flat) are present only in area 1. Areas 3 and 4 represent environments that are dominated by hemipelagic marls and allochthonous relocated platform allochems. Area 5 is not represented in this figure as there was no significant changes in facies and foraminiferal assemblages in section 5a

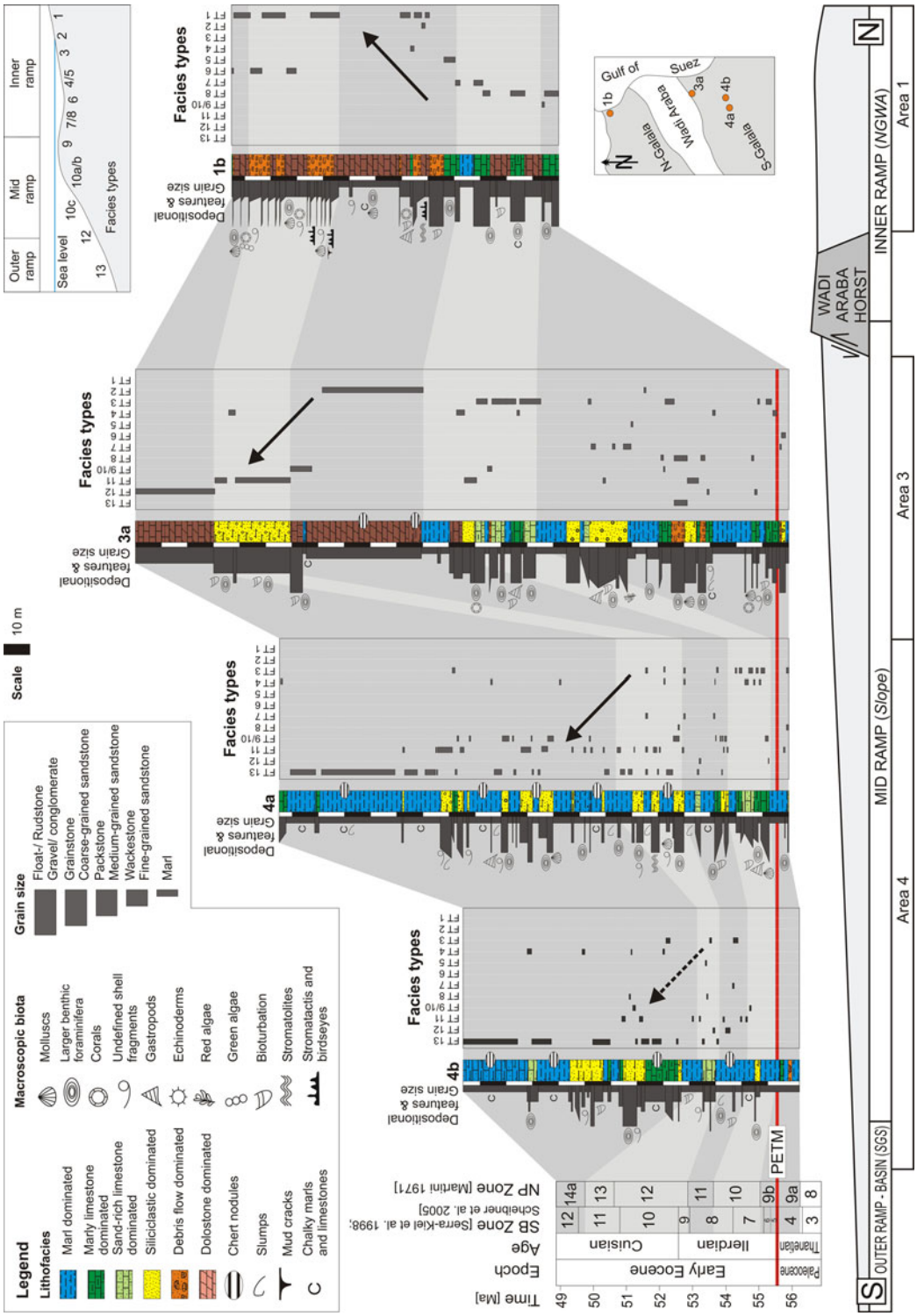

Fig. 7 Four selected sections of the lower mid ramp (sections 4a and 4b), the upper mid ramp (section 3a) and the inner ramp (section 1b) regarding FT changes during five stratigraphic intervals with the PETM (*red line*) as the base of correlation. Major lithofacies (*coloured*), grain size, macrofossils and depositional textures are added. Detailed microfacies records of the mid ramp sections indicate a shift from shallow marine environments (FT 1 to FT 5) to deep marine environments (FT 9 to FT 13) between NP 11 and NP 12/13 (*black arrows*). However, the FT of the inner ramp area indicate a shift from open lagoonal environments (FT 8) to more restricted settings with temporarily subaerial exposure (FT 1). Both diametral facies shifts are probably related to the tectonic uplift of inner ramp environments (area 1) and a coeval sea-level rise, which is represented by a deepening upward trend in the tectonically uninfluenced mid- and outer ramp areas (area 3 and 4)

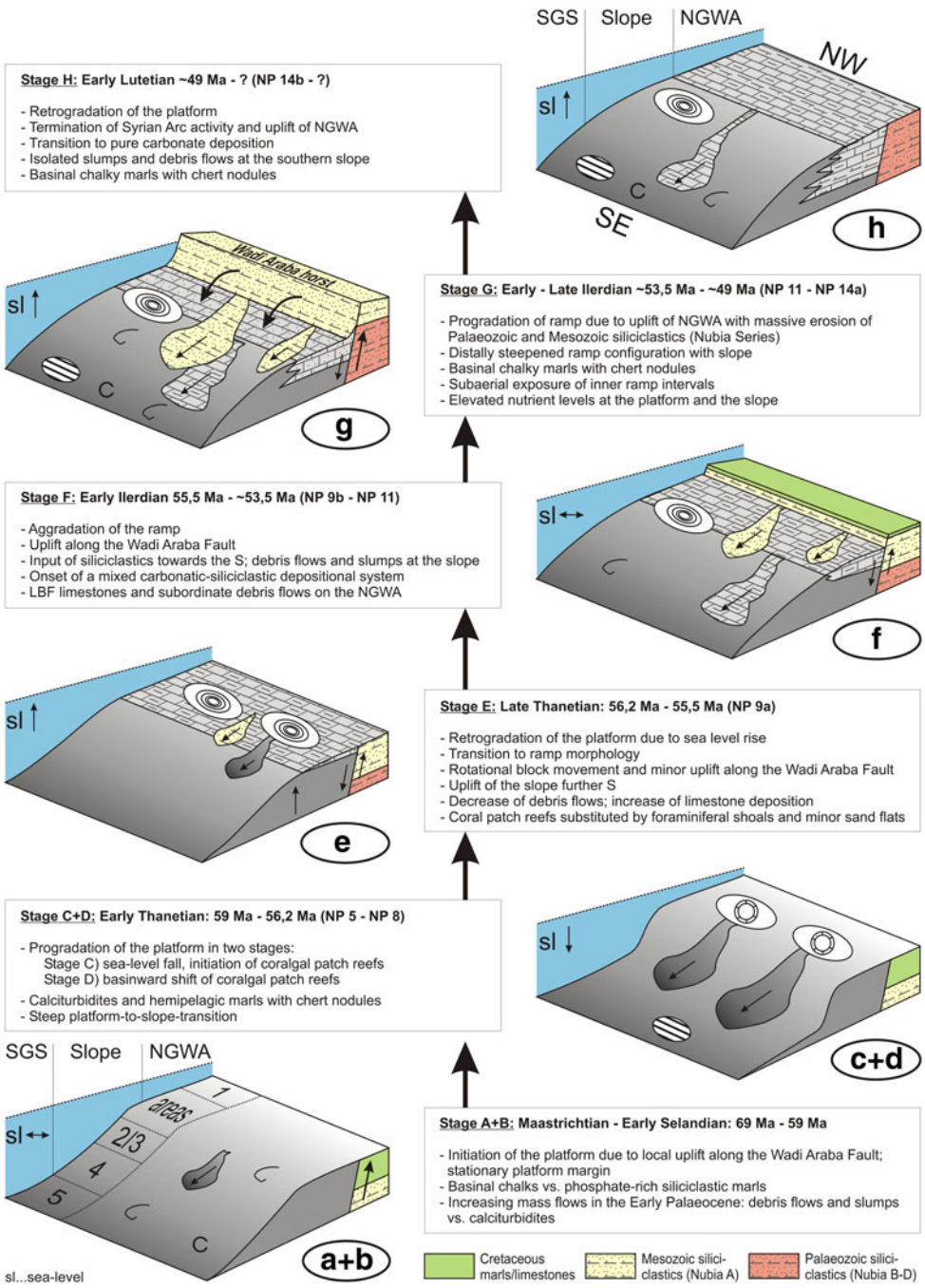

Fig. 8 Tectono-sedimentary evolution of the Galala platform from the Late Cretaceous (Maastrichtian) to the latest Early Eocene illustrated in six block schemes, which refer to eight platform stages (*A*–*H*). Platform stages *A*–*E* were described by Scheibner et al. (2003), platform stage *F* was introduced by Scheibner and Speijer (2008). Stages *G* and *H* are newly introduced in this paper. The initiation of the platform and its Early Eocene evolution were controlled by tectonic activity along the Wadi Araba Fault, which superimposed sea-level fluctuations. However, the Paleocene evolution of the platform was controlled by major sea-level fluctuations. Stage *G* is again controlled by renewed tectonic activity along the Wadi Araba Fault. In contrast to stage *G*, the activity of the Wadi Araba Fault is terminated in stage *H*. The stratigraphic range of stage *H* will be explored. For a legend of the icons used, see Fig. 7

increases, especially in the Southern Galala mid ramp sections (area 2, 3 and 4). Siliciclastic deposits from the NGWA are reported from few sections at the southern margin of the Northern Galala Plateau (Gietl 1998). At the northern margin of the NGWA, pure carbonate deposition prevailed throughout the Lower Eocene (area 1). The dominance of siliciclastic material at the Southern Galala Plateau and the coeval pure carbonate deposition at the NGWA suggest a source area of the siliciclastic material north of the Wadi Araba Fault. Furthermore, major sandstone intervals at the Southern Galala mid ramp indicate the prevailing transport direction of quartz-rich deposits towards the South.

The deposition of siliciclastics at the isolated Galala platform is related to tectonically induced uplift and erosion of older sandstones along the Wadi Araba Fault. This was confirmed by Hussein and Abd-Allah (2001), who described increased Lower Eocene oblique convergence at the unstable Egyptian shelf resulting in the reactivation of Mesozoic fault systems and the uplift along the Syrian Arc-Fold-Belt. This tectonic reactivation resulted in an uplift of Palaeozoic and Mesozoic sandstones with a vertical

displacement of more than 500 m (Schütz 1994). Hence, the sandstones, which belong to the Nubia Series (Late Carboniferous—Early Cretaceous) were subaerial exposed and eroded in the Early Eocene (Fig. 8g).

The onset of a mixed carbonate-siliciclastic depositional system at the Southern Galala Plateau during the Early Eocene is reflected by increasing contents of terrigeneous quartz grains, either as distinct beds of sandstone or as disseminated components in marls and limestones. Sandstone beds accumulate in intervals of several metres to tens of metres, which are traceable throughout area 2, 3 and 4. Generally, the correlation of the siliciclastic units on the platform to basin transect is difficult, due to highly variable thicknesses of the beds and assuming various point sources of the siliciclastic material in the vicinity of the Wadi Araba Fault (Figs. 6, 7). For this reason, the impact of various tectonic pulses is thought to be a major trigger for the relocation of quartz-rich sediments. Major tectonic activity of the Wadi Araba Fault is estimated within NP 11 and NP 14a when thick quartz-rich packages were deposited (Fig. 6). Within NP 14a, the system shifted towards pure carbonate deposition (Fig. 8h).

Conclusions

The biotic and abiotic evolution of the Early Eocene Galala platform is influenced strongly by regional tectonic uplift along the Wadi Araba Fault, superimposing the effects of eustatic sea-level fluctuations. The definition and interpretation of 13 facies types and six foraminiferal assemblages as well as qualitative analyses of dominating platform biota are demonstrated in the following results:

- The Early Eocene monoclinal uplift along the Wadi Araba Fault intensified with respect to the Paleocene and Late Cretaceous. Amalgamated intervals of siliciclastic material as well as slumps and coarse-grained debris flows indicate multiple tectonic pulses and local steep slope gradients. The heterogeneous distribution and irregular lateral extension of siliciclastics probably reflect a complex ramp topography, which is influenced by local uplift and subsidence, as well as pre-existent swells and troughs. The origin of those swells is probably related to pre-Eocene progradational platform stages. Although the overall ramp gradient does not indicate any steepening, frequent mass flow deposits at the lower mid ramp support the onset of a distally steepened ramp in the Early Eocene.
- Following previous studies of Scheibner et al. (2003) and Scheibner and Speijer (2008), we complete and expand the platform model with respect to the Early Eocene succession. Platform stage F, introduced and described by Scheibner and Speijer (2008) ranges from NP 9b to NP 11 and demonstrates a period of platform aggradation with the reactivation of the Wadi Araba Fault.
- We introduce two new platform stages regarding varying biotic and tectono-sedimentary constraints: Stage G (NP 11–NP 14a) is characterized by the repeated activity along the Wadi Araba Fault and the massive input of Palaeozoic and Mesozoic siliciclastic material towards the S. The retrogradation of the platform is demonstrated by a shift in the microfacies signature of the mid- and outer ramp succession (~NP 11/12). However, the antithetic evolution of inner ramp environments reflects a sea-level drop and the onset of tidal-related loferite cycles. This contradiction is related to the uplift of a horst structure along the Wadi Araba Fault, which formed a palaeogeographic barrier between inner- and mid ramp environments.
- In contrast to stage G, the following stage H (NP 14a) reflects the termination of tectonic activity along the Wadi Araba Fault. The horst structure initiated in stage G was completely eroded during that stage. The system shifts to pure carbonate deposition, dominated by chalky, chert-rich marls at the mid- and outer ramp. The stratigraphic range of platform stage H will be subject to further studies.

Acknowledgements The authors sincerely thank A. Freiwald (Wilhelmshaven) and an anonymous reviewer for a stimulating review of the manuscript. We thank Dr. Abdel-Mohsen Morsi and Dr. Abdel-Monem Soltan for their excellent help and organisation of our field trips in Egypt. We are grateful to Prof. Mohamed Boukhary, who has determined various nummulitids for this study. Furthermore, we thank Ralf Bätzel, Christian Sommerfeld, Patrick Simundic and Karin Gieserich for the assiduous preparation of the samples, as well as Steven P. Morrissey for his creative stimulation. This project was funded by the German Science Foundation (DFG-KU 642/221).

References

Abdallah AM, Sharkawi MAE, Marzouk A (1970) Geology of Mersa Thelmet area, southern Galala, Eastern Desert A. R. E. Bull Fac Sci, Cairo Univ 44:271–280

Adabi M, Zohdi A, Ghabeishavi A, Amiri-Bakhtiyar H (2008) Applications of nummulitids and other larger benthic foraminifera in depositional environment and sequence stratigraphy: an example from the Eocene deposits in Zagros Basin, SW Iran. Facies 54:499–512

Ahlbrandt TS (2001) The Sirte Basin Province of Libya—Sirte-Zelten total petroleum system. US Geol Surv Bull 2202-F, pp 29

Aubry MP (1995) Towards an upper Paleocene-lower Eocene high resolution stratigraphy based on calcareous nannofossil stratigraphy. Isr J Earth Sci 44:239–253

Aubry MP, Cramer BS, Miller KG, Wright JD, Kent DV, Olsson RK (2000) Late Paleocene event chronology: unconformities, not diachrony. Bull Soc Géol Fr 171:367–378

Baaske UP, Itterbeeck JV, Griffiths H, Tricker P, Mugheiry M, Burgess P (2008) The Eocene carbonate System(s) of the Sirte Basin, Libya: implications of regional-scale observations. In: Abstracts,

2008 AAPG International Conference and Exhibition, 26–29 October 2008, Cape Town, South Africa

Baccelle L, Bosellini A (1965) Diagrammi per la stima visiva della composizione percentuale nelle rocce sedimentarie. Annali dell'Università di Ferrara (Nuova Serie). Sezione IX. Sci Geol Paleontol 1:117–153

Bandel K, Kuss J (1987) Depositional environment of the pre-rift sediments—Galala Heights (Gulf of Suez, Egypt). Berl Geowiss Abh 78:1–48

Bassi D (1998) Coralline algal facies and their palaeoenvironments in the Late Eocene of Northern Italy (Calcare di Nago, Trento). Facies 39:179–202

Beadnell HJL (1905) The relations of the Eocene and Cretaceous systems in the Esna-Aswan reach of the Nile Valley. Q J Geol Soc Lond 61:667–678

Beavington-Penney SJ, Racey A (2004) Ecology of extant nummulitids and other larger benthic foraminifera: applications in palaeoenvrionmental analysis. Earth Sci Rev 67:219–265

Bechstädt T, Boni M (1989) Tectonic control on the formation of a carbonate platform: the Cambrian of Southwestern Sardinia. In: Crevello PD, Wilson JL, Sarg JF, Read JF (1989) Controls on carbonate platforms and basin development. SEPM Special Publication 44, pp 107–122

Bosellini A (1989) Dynamics of Tethyan carbonate platforms. In: Crevello PD, Wilson JL, Sarg F, Read JF (eds) Controls on carbonate platform and basin development, SEPM Special Publication 44, pp 3–13

Bosence D (2005) A genetic classification of carbonate platforms based on their basinal and tectonic settings in the Cenozoic. Sed Geol 175:49–72

Burchette TP (1988) Tectonic control on carbonate platform facies distribution and sequence development: Miocene, Gulf of Suez. Sed Geol 59:179–204

Cosovic V, Drobne K (1995) Palaeoecological significance of morphology of orthophragminids from the Istrian Peninsula. Geobios 18:93–99

Cosovic V, Drobne K, Moro A (2004) Paleoenvironmental model for Eocene foraminiferal limestones of the Adriatic carbonate platform (Istrian Peninsula). Facies 50:61–75

Davies G (1970) Carbonate bank sedimentation, eastern Shark Bay, Western Australia. Am Assoc Petrol Geol Mem 13:85–168

Dill HG, Wehner H, Kus J, Botz R, Berner Z, Stüben D, Al-Sayigh A (2007) The Eocene Rusayl formation, Oman, carbonaceous rocks in calcareous shelf sediments: environment of deposition, alteration and hydrocarbon potential. Int J Coal Geol 72:89–123

Everts AJW (1991) Interpreting compositional variations of calciturbidites in relation to platform-stratigraphy: an example from the Paleogene of SE Spain. Sediment Geol 71:231–242

Förstner U, Müller G, Reineck HE (1968) Sedimente und Sedimentgefüge des Rheindeltas im Bodensee. sediments and sedimentary structures of the Rhine delta in Lake Constance. N Jahrb Miner Abh 109:33–62

Geel T (2000) Recognition of stratigraphic sequences in carbonate platform and slope deposits: empirical models based on microfacies analysis of Palaeogene deposits in southeastern Spain. Palaeogeogr Palaeoclimatol Palaeoecol 155:211–238

Gietl R (1998) Biostratigraphie und Sedimentationsmuster einer nordostägyptischen Karbonatrampe unter Berücksichtigung der Alveolinen-Faunen. Ber Fachb Geowiss Univ Bremen 112:1–135

Hallock P (1985) Why are larger foraminifera large? Paleobiology 11:195–208

Hallock P, Glenn EC (1986) Larger foraminifera: a tool for paleoenvironmental analysis of Cenozoic carbonate depositional facies. Palaios 1:55–64

Haq BU, Hardenbol J, Vail P (1987) Chronology of fluctuating sea levels since the Triassic. Science 235:1156–1167

Hermina M, Lindenberg HG (1989) The tertiary. In: Hermina M, Klitzsch E, List FK (eds) Stratigraphic lexicon and explanatory notes to the geological map of Egypt 1:500,000. Conoco, Cairo, pp 141–217

Hohenegger J (2005) Estimation of environmental paleogradient values based on presence/absence data: a case study using benthic foraminifera for paleodepth estimation. Palaegeogr Palaeoclimatol Palaeoecol 217:115–130

Hohenegger J, Yordanova E, Nakano Y, Tatzreiter F (1999) Habitats of larger foraminifera on the upper reef slope of Sesoko Island, Okinawa, Japan. Mar Micropaleontol 36:109–168

Hottinger L (1973) Selected Paleogene larger foraminifera. In: Hallam A (ed) Atlas of palaeobiogeography. Elsevier, Amsterdam, pp 443–452

Hottinger L (1974) Alveolinids, cretaceous tertiary larger Foraminifera, Exxon Research—European laboratories. Schudel, Riehen, Switzerland, p 85

Hottinger L (1997) Shallow benthic foraminiferal assemblages as signals for depth of their deposition and their limitations. Bull Soc Géol Fr 168:491–505

Hottinger L (1998) Shallow benthic foraminifera at the Paleocene-Eocene boundary. Strata 1(9):61–64

Hottinger L, Schaub H (1960) Zur Stufeneinteilung des Paleocaens und des Eocaens. Eclogae Geol Helv 53:453–479

Hussein IM, Abd-Allah AMA (2001) Tectonic evolution of the northeastern part of the African continental margin, Egypt. J Afr Earth Sci 33:49–68

Keheila EA, El-Ayyat AAM (1990) Lower Eocene carbonate facies, environments and sedimentary cycles in Upper Egypt: evidence for global sea-level changes. Palaeogeogr Palaeoclimatol Palaeoecol 81:333–347

Keheila EA, El-Ayyat AM (1992) Silicification and dolomitization of the Lower Eocene carbonates in the Eastern Desert between Sohag and Qena, Egypt. J Afr Earth Sci 14:341–349

Krenkel E (1925) Geologie Afrikas. Bornträger, Berlin, p 461

Kuss J (1986) Facies development of Upper Cretaceous-Lower Tertiary sediments from the monastery of St. Anthony/Eastern Desert, Egypt. Facies 15:177–194

Kuss J, Leppig U (1989) The early Tertiary (middle-late Paleocene) limestones from the western Gulf of Suez, Egypt. N Jahrb Geol Paläontol Abh 177:289–332

Kuss J, Scheibner C, Gietl R (2000) Carbonate platform to basin transition along an Upper Cretaceous to Lower Tertiary Syrian Arc Uplift, Galala Plateaus, Eastern Desert, Egypt. GeoArabia 5:405–424

Lee Wilson J, D'Argenio B (1982) Controls on carbonate platforms and basin systems development. Geology 10:659–661

Lighty RG (1985) Preservation of internal reef porosity and diagenetic sealing of submerged early Holocene barrier reef, southeast Florida shelf. In: Bricker OP (ed) Carbonate cements. Johns Hopkins Press, Baltimore, pp 123–151

Loucks RG, Moody RTJ, Bellis JK, Brown AA (1998) Regional depositional setting and pore network systems of the El Garia Formation (Metlaoui Group, Lower Eocene), offshore Tunisia. In: Macgregor DS, Moody RTJ, Clark-Lowes DD (eds) Petroleum geology of North Africa. Geological Society Special Publication 132, pp 355–374

Lüning S, Marzouk AM, Kuss J (1998) The Paleocene of central East Sinai, Egypt: "sequence stratigraphy" in monotonous hemipelagites. J Foraminifer Res 28:19–39

Luterbacher H (1984) Paleoecology of foraminifera in the Paleogene of the southern Pyrenees. Benthos′83, 2nd Int Symp Benthic Foraminifera, pp 389–392

Martini E (1971) Standard Tertiary and Quaternary calcareous nannoplankton zonation. In: Farinacci A (ed) Proc II Plankton Conf, Roma, Ed Tecnosci Rome, Roma, pp 739–785

McBride EF, Abdel-Wahab A, El-Younsy ARM (1999) Origin of spheroidal chert nodules, Drunka Formation (Lower Eocene), Egypt. Sedimentology 46:733–755

Meshref WM (1990) Tectonic framework. In: Said R (ed) The geology of Egypt. Balkema, Rotterdam, pp 113–156

Miller KG, Kominz MA, Browning JV, Wright JD, Mountain GS, Katz ME, Sugarman PJ, Cramer BS, Christie-Blick N, Pekar SF (2005) The Phanerozoic record of global sea-level change. Science 310:1293–1298

Morsi AMM, Scheibner C (2009) Paleocene—Early Eocene ostracodes from the Southern Galala Plateau (Eastern Desert, Egypt): taxonomy, impact of paleobathymetric changes. Rev Micropaléontol 52:149–192

Moustafa AR, El-Rey AK (1993) Structural characteristics of the Suez rift margins. Geol Rundschau 82:101–109

Moustafa AR, Khalil MH (1995) Superposed deformation in the northern Suez Rift, Egypt: relevance to hydrocarbons exploration. J Petrol Geol 18:245–266

Murray JW (1991) Ecology and paleoecology of benthic Foraminifera. Longman, New York

Orue-Etxebarria X, Pujalte V, Bernaola G, Apellaniz E, Baceta JI, Payros A, Nunez-Betelu K, Serra-Kiel J, Tosquella J (2001) Did the Late Paleocene thermal maximum affect the evolution of larger foraminifers? Evidence from calcareous plankton of the Campo Section (Pyrenees, Spain). Mar Micropal 41:45–71

Özgen-Erdem N, Inan N, Ajyazi M, Tunoglu C (2005) Benthonic foraminiferal assemblages and microfacies analysis of Paleocene-Eocene carbonate rocks in the Kastamonu region, Northern Turkey. J Asian Earth Sci 25:403–417

Papazzoni C, Trevisani E (2006) Facies analysis, palaeoenvironmental reconstruction, and biostratigraphy of the "Pesciara di Bolca" (Verona, northern Italy): an early Eocene Fossil-Lagerstätte. Palaeogeogr Palaeoclimatol Palaeoecol 242:21–35

Pearson PN, van Dongen BE, Nicholas CJ, Pancost RD, Schouten S, Singano JM, Wade BS (2007) Stable warm tropical climate through the Eocene Epoch. Geology 35:211–214

Pujalte V, Baceta JI, Payros A, Orue-Etxebarria X, Schmitz B (1999) Upper Paleocene-Lower Eocene strata of the W. Pyrenees, Spain: a shelf-to-basin correlation. In: Andreasson FP, Schmitz B, Thompson EI (eds) Early Paleogene warm climates and biosphere dynamics. Dep Mar Geol, Göteborg

Pujalte V, Schmitz B, Baceta JI, Orue-Etxebarria X, Bernaola G, Dinares-Turell J, Payros A, Apellaniz E, Caballero F (2009) Correlation of the Thanetian-Illerdian turnover of larger foraminifera and the Paleocene-Eocene thermal maximum: confirming evidence from the Campo area (Pyrenees, Spain). Geol Acta 7:161–175

Racey A (1994) Biostratigraphy and palaeobiogeographic significance of Tertiary nummulitids (Foraminifera) from northern Oman. In: Simmons MD (ed) Micropalaeontology and hydrocarbon exploration in the Middle East. Chapman and Hall, London, pp 343–367

Rasser MW (1994) Facies and palaeoecology of rhodoliths and acervulinid macroids in the Eocene of the Krappfeld (Austria). Beitr Paläontol 19:191–217

Rasser MW, Scheibner C, Mutti M (2005) A paleoenvironmental standard section for Lower Ilerdian tropical carbonate factories (Pyrenees, Spain; Corbieres, France). Facies 51:217–232

Rea DK, Zachos JC, Owen RM, Gingerich PD (1990) Global change at the Paleocene-Eocene boundary: climatic and evolutionary consequences of tectonic events. Palaegeogr Palaeoclimatol Palaeoecol 79:117–128

Reineck HE, Singh IB (1980) Depositional sedimentary environments, 2nd edn. Springer, Berlin

Renema W (2006) Large benthic foraminifera from the deep photic zone of a mixed siliciclastic-carbonate shelf off East Kalimantan, Indonesia. Mar Micropaleontol 58:73–82

Said R (1990) Cenozoic. In: Said R (ed) The geology of Egypt. Balkema, Rotterdam, pp 451–486

Salem R (1976) Evolution of Eocene-Miocene sedimentation patterns in parts of northern Egypt. AAPG Bull 60:34–64

Schäfer K (1969) Vergleichs-Schaubilder zur Bestimmung des Allochemgehalts bioklastischer Karbonatgesteine. N Jahrb Geol Paläontol Monatshefte 1969:173–184

Schaub H (1992) The Campo Section (NE Spain) a Tethyan parastratotype of the Cuisian. N Jahrb Geol Paläontol Abh 186:63–70

Scheibner C, Speijer RP (2008) Late Paleocene–early Eocene Tethyan carbonate platform evolution—a response to long- and short-term paleoclimatic change. Earth Sci Rev 90:71–102

Scheibner C, Speijer RP (2009) Recalibration of the Tethyan shallow-benthic zonation across the Paleocene-Eocene boundary; the Egyptian record. Geol Acta 7:195–214

Scheibner C, Kuss J, Marzouk AM (2000) Slope sediments of a Paleocene ramp-to-basin transition in NE Egypt. Int J Earth Sci 88:708–724

Scheibner C, Marzouk AM, Kuss J (2001a) Maastrichtian-Early Eocene litho- biostratigraphy and palaeogeography of the northern Gulf of Suez region, Egypt. J Afr Earth Sci 32:223–255

Scheibner C, Marzouk AM, Kuss J (2001b) Shelf architectures of an isolated Late Cretaceous carbonate platform margin, Galala Mountains (Eastern Desert, Egypt). Sediment Geol 145:23–43

Scheibner C, Kuss J, Speijer RP (2003) Stratigraphic modelling of carbonate platform-to-basin sediments (Maastrichtian to Paleocene) in the Eastern Desert, Egypt. Palaeogeogr Palaeoclimatol Palaeoecol 200:163–185

Scheibner C, Speijer RP, Marzouk AM (2005) Larger foraminiferal turnover during the Paleocene/Eocene thermal maximum and paleoclimatic control on the evolution of platform ecosystems. Geology 33:493–496

Scheibner C, Rasser MW, Mutti M (2007) Facies changes across the Paleocene-Eocene boundary: The Campo section (Pyrenees, Spain) revisited. Palaegeogr Palaeoclimatol Palaeoecol 248:145–168

Schütz KI (1994) Structure and stratigraphy of the Gulf of Suez, Egypt. In: Landon SM (ed) Interior rift basins, AAPG Memoir 59, pp 57–96

Serra-Kiel J, Hottinger L, Caus E, Drobne K, Ferrandez C, Jauhri AK, Less G, Pavlovec R, Pignatti J, Samso JM, Schaub H, Sirel E, Strougo A, Tambareau Y, Tosquella J, Zakrevskaya E (1998) Larger foraminiferal biostratigraphy of the Tethyan Paleocene and Eocene. Bull Soc Géol Fr 169:281–299

Shahar J (1994) The Syrian Arc System: an overview. Palaeogeogr Palaeoclimatol Palaeoecol 112:125–142

Speijer RP, Schmitz B (1998) A benthic foraminiferal record of Paleocene sea level and trophic/redox conditions at Gebel Aweina, Egypt. Palaeogeogr Palaeoclimatol Palaeoecol 137:79–101

Speijer RP, Wagner R (2002) Sea-level changes and black shales associated with the late Paleocene thermal maximum; organic-geochemical and micropaleontologic evidence from the southern Tethyan margin (Egypt-Israel). In: Koeberl C, MacLeod KG (eds) Catastrophic events & mass extinctions: impacts and beyond. Geological Society of America Special Paper 356, Geological Society of America, Boulder, pp 533–549

Strougo A, Faris M (1993) Paleocene-Eocene stratigraphy of Wadi El Dakhl, Southern Galala plateau. Middle East Research Center, Ain Shams University, Earth Sciences Series, vol 7, pp 49–62

Tripati AK, Delaney ML, Zachos JC, Anderson LD, Kelly DC, Elderfield H (2003) Tropical sea-surface temperature reconstruction for the early Paleogene using Mg/Ca ratios of planktonic foraminifera. Paleoceanography 18:1101. doi:1110.1029/2003PA000937, 002003

Werner J (1963) Über die Bedeutung der Opal-Phytolithen als Mikrofossilien des Bodens. Eiszeitalter Gegenwart 14:229

Wielandt U (1996) Benthic foraminiferal paleoecology and microfacies investigations of Paleogene sediments from the Farafra Oasis, Western Desert, Egypt. Tübinger Mikropaläontol Mitt 13:1–78

Youssef MM (2003) Structural setting of central and south Egypt: an overview. Micropaleontology 49:1–13

Zachos JC, Stott LD, Lohmann KC (1994) Evolution of early Cenozoic marine temperatures. Paleoceanography 9:353–387

Zachos J, Pagani M, Sloan L, Thomas E, Billups K (2001) Trends, rhythms, and aberrations in global climate 65 Ma to present. Science 292:686–693

Zachos JC, Dickens GR, Zeebe RE (2008) An early Cenozoic perspective on greenhouse warming and carbon-cycle dynamics. Nature 451:279–283

Zamagni J, Mutti M, Kosir A (2008) Evolution of shallow benthic communities during the Late Paleocene-earliest Eocene transition in the Northern Tethys (SW Slovenia). Facies 54:25–43